

THE CONDITION NUMBER OF RIEMANNIAN APPROXIMATION PROBLEMS

PAUL BREIDING AND NICK VANNIEUWENHOVEN

ABSTRACT. We consider the local sensitivity of least-squares problems for inverse problems. We assume that the sets of inputs and outputs of the inverse problem have the structures of Riemannian manifolds. The problems we consider include the approximation problem of finding the nearest point on a Riemannian embedded submanifold to a given point in the ambient space. We characterize the first-order sensitivity, i.e., condition number, of local minimizers and critical points to arbitrary perturbations of the input of the least-squares problem. This condition number involves the Weingarten map of the input manifold. We validate our main results through experiments with the n -camera triangulation problem in computer vision.

1. INTRODUCTION

A prototypical instance of the Riemannian optimization problems we consider here is the following inverse problem (IP): given an input $x \in \mathcal{I}$, compute $y \in \mathcal{O}$ such that $F(y) = x$. Herein, we are given a *system* modeled as a smooth map F between a Riemannian manifold \mathcal{O} , the *output manifold*, and a Riemannian embedded submanifold $\mathcal{I} \subset \mathbb{R}^n$, the *input manifold*. If $a = x + \Delta x \in \mathbb{R}^n$ is a perturbation of the input data x we attempt to solve the following least squares problem associated to the IP above.

$$\text{(PIP)} \quad \arg \min_{y \in \mathcal{O}} \|a - F(y)\|^2.$$

In [7] we called this type of problem a *parameter identification problem* (PIP).

The manifold \mathcal{O} is called output manifold because its elements are the outputs of the optimization problem. The outputs are the quantities of interest; for instance, they could be the unknown parameters that one wants to identify based on a given observation x and the forward description of the system (or model) F . In this paper, we consider the sensitivity of the output of the optimization problem (PIP) when the input a is perturbed by studying its *condition number* κ at global and local minimizers and critical points. In fact, we will consider a slightly more general version of (PIP), where an input $x \in \mathcal{I}$ may have several outputs $y \in \mathcal{O}$.

In the experimental section below, we compute the condition of PIPs in computer vision [17, 18, 29]. Other application areas where PIPs originate are low-rank matrix and tensor decompositions for data completion [8, 11, 22, 41, 44] or geometric modeling [10, 27, 42].

1.1. The condition number. Condition numbers are a central concept in numerical analysis [5, 9, 20]. The classic definition of condition numbers was extended to Riemannian manifolds already in the early days of numerical analysis. In 1966, Rice [34] presented the definition in the case where input and output space are general nonlinear *metric spaces*; the special case of *Riemannian manifolds* he stated in [34, Theorem 3]. Assume that \mathcal{I} and \mathcal{O} are Riemannian manifolds and that

$F : \mathcal{O} \rightarrow \mathcal{I}$ is invertible with inverse $f : \mathcal{I} \rightarrow \mathcal{O}$. Then, Rice's definition of condition at a point $x \in \mathcal{I}$ is

$$(1) \quad \kappa[f](x) := \lim_{\epsilon \rightarrow 0} \sup_{\substack{x' \in \mathcal{I}, \\ d_{\mathcal{I}}(x, x') \leq \epsilon}} \frac{d_{\mathcal{O}}(f(x), f(x'))}{d_{\mathcal{I}}(x, x')},$$

where $d_{\mathcal{I}}(\cdot, \cdot)$ denotes the distance given by the Riemannian metric on \mathcal{I} and likewise for \mathcal{O} . The number $\kappa[f](x)$ is called the *absolute* condition number. On the other hand, the *relative* condition number is $\kappa_{\text{rel}}[f](x) := \kappa[f](x) \frac{\|x\|_{\mathcal{I}}}{\|f(x)\|_{\mathcal{O}}}$. We focus on computing the absolute condition number, but emphasize that the relative condition number can be inferred from the absolute one.

It follows from (1) that the condition number yields an asymptotically sharp upper bound on the perturbation of the output of a computational problem when subjected to a perturbation of the input x . Indeed, we have

$$\text{dist}_{\mathcal{O}}(f(x), f(x')) \leq \kappa(x) \|x - x'\|_2 + o(\|x - x'\|),$$

where $\text{dist}_{\mathcal{O}}(y, y')$ is the Riemannian distance between y and y' . The condition number quantifies the sensitivity of outputs to perturbations of x accordingly.

Rice's definition cannot be applied unreservedly to (PIP). There are two issues: First, requiring that the systems in (PIP) can be modeled by an invertible function $F : \mathcal{O} \rightarrow \mathcal{I}$ excludes many interesting computational problems. For example, computing the eigenvalues of a symmetric matrix cannot be modeled as a map from outputs to inputs: there are infinitely many symmetric matrices with a prescribed set of eigenvalues. Second, more fundamentally, if we want to apply Rice's result to (PIP), we have to take \mathbb{R}^n to be the input space in (1). This is because the input data $a \in \mathbb{R}^n$ is not constrained to be in \mathcal{I} . However, sending a to the solution of (PIP) is not a smooth map in general. There could be several global minimizers for a fixed a . For our theory to be practical, we need to consider the condition number of every minimizer separately. Exceeding this goal, we will present the condition number of each critical point in this paper. This also takes into account that nonconvex optimization problems like (PIP) are difficult to solve globally, so we should realistically only expect to find local minimizers in practice.

As Wilkinson [47] and later Woźniakowski [48] realized, a solution to the first issue consists of using *local* maps. This approach was given a geometric framework by Shub and Smale in their series of papers on Bézout's theorem [35–39]; see also the books by Blum, Cucker, Shub and Smale [6] and Bürgisser and Cucker [9]. The idea is to abandon explicit maps like $F : \mathcal{O} \rightarrow \mathcal{I}$ and instead formulate the problem implicitly.

The solution of the second issue forms the heart of this paper and is addressed in Section 3 to 7. In resolving it, the implicit Shub–Smale framework is a key ingredient. We briefly recall its main points next.

1.2. Implicit computational problems. An inverse problem with input manifold \mathcal{I} and output manifold \mathcal{O} can be modeled implicitly via the so-called *solution manifold*:

$$\mathcal{S} \subset \mathcal{I} \times \mathcal{O}.$$

The problem when given an input $x \in \mathcal{I}$ is finding a corresponding output $y \in \mathcal{O}$ such that $(x, y) \in \mathcal{S}$. Since \mathcal{S} models a computational problem, we can consider the latter's condition number. Now it is defined at $(x, y) \in \mathcal{S}$ and not only at the input x , because the sensitivity to perturbations in the output depends on which output is considered.

Following [6, 9] we first define the condition number associated to \mathcal{S} for perturbations $x' = x + \Delta x$ such that $x' \in \mathcal{I}$. This definition is indispensable for defining a condition number for general perturbations $a = x + \Delta x \in \mathbb{R}^n$.

The definition given in [6, 9] is as follows: let $\pi_{\mathcal{I}} : \mathcal{S} \rightarrow \mathcal{I}$ and $\pi_{\mathcal{O}} : \mathcal{S} \rightarrow \mathcal{O}$ be the projections on the input and output manifolds, respectively. We will assume that $\dim \mathcal{S} = \dim \mathcal{I}$, because otherwise almost all inputs x have infinitely many outputs ($\dim \mathcal{S} > \dim \mathcal{I}$) or no outputs ($\dim \mathcal{S} < \dim \mathcal{I}$). Furthermore, we will assume that $\pi_{\mathcal{I}}$ is surjective, which means that every input $x \in \mathcal{I}$ has at least one output. When $D_{(x,y)}\pi_{\mathcal{I}}$ is invertible, the inverse function theorem [25, Theorem 4.5] implies that $\pi_{\mathcal{I}}$ is locally invertible. Hence, there is a local smooth *solution map* $\pi_{\mathcal{O}} \circ \pi_{\mathcal{I}}^{-1}$, which locally around (x, y) makes the computational problem explicit. This local map has a condition number as above, so that it is sensible to define

$$(2) \quad \kappa(x, y) = \begin{cases} \kappa[\pi_{\mathcal{O}} \circ \pi_{\mathcal{I}}^{-1}](x) & \text{if } D_{(x,y)}\pi_{\mathcal{I}} \text{ is invertible,} \\ \infty & \text{otherwise.} \end{cases}$$

In particular, if there is an explicit smooth map $f : \mathcal{I} \rightarrow \mathcal{O}$, such that \mathcal{S} is the graph of f , then (2) reduces to Rice's definition from (1).

The points in the set $\mathcal{W} := \{(x, y) \in \mathcal{S} \mid \kappa(x, y) < \infty\}$ are called *well-posed tuples*. Points in $\mathcal{S} \setminus \mathcal{W}$ are called *ill-posed tuples*. An infinitesimally small perturbation in the input x of an ill-posed tuple (x, y) can cause an arbitrary change in the output y . It is therefore natural to assume that $\mathcal{W} \neq \emptyset$, because otherwise the computational problem is ill-posed for all inputs. If there exists $(x, y) \in \mathcal{W}$, it follows from the inverse function theorem that \mathcal{W} is an open submanifold of \mathcal{S} , so $\dim \mathcal{S} = \dim \mathcal{W}$. We will also assume that \mathcal{W} is dense. Otherwise, since \mathcal{S} is Hausdorff, around any data point outside of $\overline{\mathcal{W}}$ there would be an open neighborhood on which the computational problem is ill-posed. We argue that these input-output pairs should be removed from the definition of the problem.

In summary, we make the following assumptions in this paper.

Assumption 1. *The m -dimensional input manifold \mathcal{I} is a Riemannian embedded smooth submanifold of \mathbb{R}^n equipped with the standard Euclidean inner product from \mathbb{R}^n as Riemannian metric. The output manifold \mathcal{O} is smooth Riemannian manifold. The solution manifold $\mathcal{S} \subset \mathcal{I} \times \mathcal{O}$ is a smoothly embedded m -dimensional submanifold. The projection $\pi_{\mathcal{I}} : \mathcal{S} \rightarrow \mathcal{I}$ is surjective. The well-posed tuples \mathcal{W} form an open dense embedded submanifold of \mathcal{S} .*

The requirement that \mathcal{S} is an embedded submanifold is typically not stringent. It is satisfied for example if \mathcal{S} is the graph of a smooth map $f : \mathcal{I} \rightarrow \mathcal{O}$ or $F : \mathcal{O} \rightarrow \mathcal{I}$ (as for IPs) by [25, Proposition 5.7]. Another example is when \mathcal{S} is the smooth locus of an algebraic subvariety of $\mathcal{I} \times \mathcal{O}$, as most problems in [9]. Moreover, the condition of an input-output pair (x, y) is a local property. Since every immersed submanifold is locally embedded (see [25, Proposition 5.22]), taking a restriction of the computational problem \mathcal{S} to a neighborhood of (x, y) , in its topology as immersed submanifold, yields an embedded submanifold. The proposed theory always applies in this regard.

1.3. Main contributions. We compute the condition numbers of global minimizers, local minimizers, and critical points of the implicit generalization of (PIP):

$$(IPIP) \quad \pi_{\mathcal{O}} \circ \arg \min_{(x,y) \in \mathcal{S}} \frac{1}{2} \|a - \pi_{\mathcal{I}}(x, y)\|^2,$$

where $a \in \mathbb{R}^n$ is a given input and the norm is the Euclidean norm. We call this implicit formulation of (PIP) a Riemannian implicit PIP.

Our main contributions are contained in three theorems below. The simplest case deals with the condition number of (IPIP) at global minimizers when a is sufficiently close to the input manifold; this is stated in Theorem 1. The condition number of all critical points of a particularly important special case of (IPIP) and (PIP), namely the Riemannian approximation problem $\min_{x \in \mathcal{O}} \|a - x\|^2$, is

treated in Theorem 2. Finally, the most general case is Theorem 3: it gives the condition number of (IPIP) at all critical points.

Aforementioned theorems will show that the way in which the input manifold \mathcal{I} curves in its ambient space \mathbb{R}^n , as measured by classic differential invariants, enters the picture. To the best of our knowledge, the role of curvature in the theory of condition of smooth computational problems involving approximation was not previously identified. We see this is as one of the main contributions of this article.

1.4. Approximation versus decomposition problems. The results of this paper raise a pertinent practical question: If one has a computational problem modeled by a solution manifold \mathcal{S} that is solved via an optimization formulation as in (IPIP), which condition number is appropriate? The one of the idealized computational problem, where the input manifold in (1) is \mathcal{I} and perturbations are constrained to be tangent to \mathcal{I} ? Or the more complicated condition number of the optimization formulation, where we allow input data to be outside of \mathcal{I} and model the input space as \mathbb{R}^n ? We argue that the choice is only an illusion.

The first approach should be taken if the problem is *defined* implicitly by a solution manifold $\mathcal{S} \subset \mathcal{I} \times \mathcal{O}$ and the data are perturbations $a \in \mathbb{R}^n$ of inputs $x \in \mathcal{I}$. The idealized framework still applies because of Corollary 2. Consider for example the n -camera triangulation problem, discussed in Section 8, where the problem \mathcal{S}_{MV} (MV stands for multiview) is defined by computing the inverse of the camera projection process. If the measurements a were taken with a perfect pinhole camera for which the theoretical model is exact, then even when $a \notin \mathcal{I}_{\text{MV}}$ (e.g., errors caused by pixelization), as long as it is a sufficiently small perturbation of some $x \in \mathcal{I}_{\text{MV}}$, the first approach is suited.

On the other hand, if it is only *postulated* that the computational problem can be well approximated by the *idealized problem* \mathcal{S} , then, we argue, the newly proposed framework for Riemannian approximation problems is the more appropriate choice. In this case, the “perturbation” to the input is a modeling error. An example of this is applying n -camera triangulation to images obtained by cameras with lenses, i.e., most real-world cameras. In this case, the computational problem is not \mathcal{S}_{MV} , but rather a much more complicated problem that takes into account lens distortions. When using \mathcal{S}_{MV} as a proxy, as is usual [17, 18, 29], the computational problem becomes an optimization problem. Curvature should be taken into account then, as developed here.

1.5. Outline. Before developing the main theory, we briefly recall the necessary concepts from differential geometry. Of particular importance are the second fundamental form and Weingarten map, which will be our main protagonists. The theory of condition of (IPIP) is first stated in Section 3 for the special case of unique global minimizers. Thereafter, in Section 4, we transition to studying critical points. Section 4 derives the condition number of the special case where the solution manifold is the identity map, i.e., Riemannian approximation problems, while Section 5 treats the general case. The condition numbers in Section 3 to 5 are derived from implicit formulations of the Riemannian IPIPs. For additional clarity, in the case of local minimizers, we also express them as condition numbers of global minimizers of localized Riemannian optimization problems in Section 6. The main ingredient in the proofs of aforementioned results is developed in Section 7. The paper is concluded with an application of our theory to the triangulation problem in multiview geometry in Section 8.

1.6. Notation. The identity map $\mathbf{1}_{\mathcal{M}} : \mathcal{M} \rightarrow \mathcal{M}$ is denoted by $\mathbf{1}$ throughout, the space on which it is the identity being clear from the context.

2. PRELIMINARIES FROM DIFFERENTIAL GEOMETRY

We briefly recall the main concepts from differential and Riemannian geometry that we will use. The notation introduced here will be used throughout the paper. Proofs of the fundamental results appearing below can be found in books such as [14, 24, 25, 30–32]. Readers familiar with these references can safely jump forward to the next section.

2.1. Manifolds. By *smooth n -dimensional manifold* \mathcal{M} we mean a C^∞ topological manifold that is second-countable, Hausdorff, and locally Euclidean of dimension n . The tangent space $T_p\mathcal{M}$ is the n -dimensional linear subspace of *differential operators at p* . A differential operator at $p \in \mathcal{M}$ is a linear map v_p from the vector space $C^\infty(\mathcal{M})$ over \mathbb{R} of smooth functions $f : \mathcal{M} \rightarrow \mathbb{R}$ to \mathbb{R} that satisfies the product rule: $v_p(f \cdot g) = (v_p f) \cdot g(p) + f(p) \cdot (v_p g)$ for all $f, g \in C^\infty(\mathcal{M})$. If $\mathcal{M}^m \subset \mathbb{R}^n$ is *embedded*, an equivalent definition of the tangent space is as the linear span of $\frac{d}{dt}|_{t=0}\gamma(t)$ where $\gamma \subset \mathcal{M}$ is a smooth curve passing through p at 0. The identification of $\frac{d}{dt}|_{t=0}\gamma(t)$ as a differential operator is $v_1\partial_1 + \dots + v_n\partial_n$, where $\frac{d}{dt}|_{t=0}\gamma(t)\gamma(t) = (v_1, \dots, v_n)$ and where $\partial_i x_j = \delta_{i,j}$, the Kronecker delta, and x_j are coordinates on \mathbb{R}^n .

A differentiable map $F : \mathcal{M} \rightarrow \mathcal{N}$ induces a linear map between tangent spaces $D_p F : T_p\mathcal{M} \rightarrow T_{F(p)}\mathcal{N}$, called the *derivative* of F at p . If $v_p \in T_p\mathcal{M}$, then $w_{F(p)} := (D_p F)(v_p)$ is the differential operator $w_{F(p)}(f) := v_p(f \circ F)$ for all $f \in C^\infty(\mathcal{N})$.

2.2. Riemannian manifolds. *Riemannian manifolds* are smooth manifolds \mathcal{M} equipped with an additional structure: a *Riemannian metric* g , which defines a positive definite symmetric bilinear form $g_p : T_p\mathcal{M} \times T_p\mathcal{M} \rightarrow \mathbb{R}$ that varies smoothly with p . The metric g_p induces a norm on $T_p\mathcal{M}$ denoted $\|t_p\|_{\mathcal{M}} := \sqrt{g_p(t_p, t_p)}$. The only Riemannian metric we will explicitly use in computations is the standard Riemannian metric of \mathbb{R}^n , i.e., the Euclidean inner product $g_p(x, y) = \langle x, y \rangle = x^T y$.

If \mathcal{M} and \mathcal{N} are Riemannian manifolds with induced norms $\|\cdot\|_{\mathcal{M}}$ and $\|\cdot\|_{\mathcal{N}}$, and if $F : \mathcal{M} \rightarrow \mathcal{N}$ is a differentiable map, then the spectral norm of the derivative of F at p is

$$\|D_p F\|_{\mathcal{M} \rightarrow \mathcal{N}} := \sup_{t_p \in T_p\mathcal{M} \setminus \{0\}} \frac{\|(D_p F)(t_p)\|_{\mathcal{N}}}{\|t_p\|_{\mathcal{M}}}.$$

If the manifolds are clear from the context we sometimes drop the subscript and write $\|D_p F\|$.

2.3. Tubular neighborhoods. Let $\mathcal{M}^m \subset \mathbb{R}^n$ be an embedded submanifold. The disjoint union of tangent spaces to \mathcal{M}^m is the *tangent bundle* of \mathcal{M} :

$$T\mathcal{M} := \coprod_{p \in \mathcal{M}} T_p\mathcal{M} = \{(p, v) \mid p \in \mathcal{M} \text{ and } v \in T_p\mathcal{M}\}.$$

The tangent bundle is a smooth manifold of dimension $2n$. The *normal bundle* is constructed similarly. Recall that the *normal space* of \mathcal{M} in \mathbb{R}^n at p is the orthogonal complement in \mathbb{R}^n of the tangent space $T_p\mathcal{M}$, namely $N_p\mathcal{M} := (T_p\mathbb{R}^n)^\perp$. The normal bundle is a smooth embedded submanifold of $\mathbb{R}^n \times \mathbb{R}^n$ of dimension n . Formally, we write

$$N\mathcal{M} := \coprod_{p \in \mathcal{M}} N_p\mathcal{M} = \{(p, \eta) \mid p \in \mathcal{M} \text{ and } \eta \in N_p\mathcal{M}\}.$$

The map $E : N\mathcal{M} \rightarrow \mathbb{R}^n$, $(p, \eta) \mapsto p + \eta$ is smooth— η is a vector attached at p , so the addition is well defined. Let $\delta : \mathcal{M} \rightarrow \mathbb{R}_+$ be a positive continuous function. Consider the following open neighborhood of the normal bundle:

$$(3) \quad \mathcal{V}_\delta = \{(p, \eta) \in N\mathcal{M} \mid \|\eta\| < \delta(p)\},$$

where the norm is the one induced from the Riemannian metric; in our setting it is the standard norm on \mathbb{R}^n . There exists a δ such that the restriction $E|_{\mathcal{V}_\delta}$ becomes a diffeomorphism onto its image [25, Theorem 6.24]. Consequently, $\mathcal{T} = E(\mathcal{V}_\delta)$ is an n -dimensional, open, smooth, embedded submanifold of \mathbb{R}^n that is additionally a neighborhood of \mathcal{M} . The submanifold \mathcal{T} is called a *tubular neighborhood* of \mathcal{M} .

2.4. Vector fields and affine connections. A *smooth vector field* is a smooth map $X : \mathcal{M} \rightarrow T\mathcal{M}$ from the manifold to its tangent bundle taking a point p to a tangent vector v . By the notation $X|_p$ we mean $X(p)$. A vector field X on a properly embedded submanifold $\mathcal{M} \subseteq \mathcal{N}$ can be extended to a smooth vector field \widehat{X} on \mathcal{N} such that it agrees on \mathcal{M} : $\widehat{X}|_{\mathcal{M}} = X$. A vector field X can be multiplied by a function f as follows $(fX)|_p := f(p)X|_p$.

A *smooth frame* of \mathcal{M}^m is a tuple of m smooth vector fields (X_1, \dots, X_m) that are linearly independent: $(X_1|_p, \dots, X_m|_p)$ is a linearly independent set for all $p \in \mathcal{M}$. If these tangent vectors are moreover orthonormal for all p , then the frame is called orthonormal.

Let X be a smooth vector field on \mathcal{M} . An *integral curve* of X is a smooth curve, i.e., the image of a smooth map $\gamma : (-1, 1) \rightarrow \mathcal{M}$, such that $D_t\gamma = X|_{\gamma(t)}$ for all $t \in (-1, 1)$. For every $p \in \mathcal{M}$ the smooth vector field X generates an integral curve γ with starting point $p = \gamma(0)$. The above implies that on a smooth manifold \mathcal{M}^m , $m > 1$, there is a smooth (integral) curve *realizing* a tangent vector $v \in T_p\mathcal{M}$; that is, a curve γ such that $p = \gamma(0)$ and $v = D_0\gamma$.

A central operation we need are derivatives of vector fields, more specifically *covariant derivatives*. Let $\mathcal{X}(\mathcal{M})$ denote the set of smooth vector fields on \mathcal{M} . An *affine connection* is a map

$$\nabla : \mathcal{X}(\mathcal{M}) \times \mathcal{X}(\mathcal{M}) \rightarrow \mathcal{X}(\mathcal{M}), \quad (X, Y) \mapsto \nabla_X Y$$

that satisfies (i) $\nabla_{(fX+gY)}Z = f\nabla_X Z + g\nabla_Y Z$, (ii) $\nabla_X(fY) = f\nabla_X Y + X(f)Y$, and (iii) $\nabla_X(\alpha Y + \beta Z) = \alpha\nabla_X Y + \beta\nabla_X Z$ for all $X, Y, Z \in \mathcal{X}(\mathcal{M})$, $f, g \in C^\infty(\mathcal{M})$ and $\alpha, \beta \in \mathbb{R}$. A vector field X can act on f because tangent vectors are differential operators. The value of $\nabla_X Y$ at p is determined completely by the direction of the vector field X at p and the values of Y . Specifically, we have $(\nabla_X Y)|_p = \nabla_{X|_p} Y$ by [24, Lemma 4.2].

2.5. Levi–Civita connection. For Riemannian manifolds (\mathcal{M}, g) , it is desirable that the affine connection is *consistent* with the Riemannian metric g , such that

$$\nabla_X g(Y, Z) = g(\nabla_X Y, Z) + g(Y, \nabla_X Z), \quad \text{for all } X, Y, Z \in \mathcal{X}(\mathcal{M}).$$

A connection is *symmetric* if $\nabla_X Y - \nabla_Y X = XY - YX$. A Riemannian manifold has a unique symmetric affine connection that is compatible with the metric; it is called the *Levi–Civita connection*. The Levi–Civita connection for Riemannian embedded submanifolds $\mathcal{M} \subset \mathbb{R}^n$ equipped with the inherited metric is the *Euclidean connection* $\widetilde{\nabla}_X Y := \sum_{i=1}^n (X y_i) \partial_i$, where the $y_i \in C^\infty(\mathcal{M})$, X acts on y_i by differentiation, and the ∂_i are the differential operators defining a basis for $T_p\mathbb{R}^n$ at every point p . In our examples, we will compute the covariant derivative $\widetilde{\nabla}_X Y$, with $X, Y \in \mathcal{X}(\mathcal{M})$, using the classical derivative, as follows:

$$(\widetilde{\nabla}_X Y)|_p = \widetilde{\nabla}_{X|_p} Y = \frac{d}{dt} Y|_{\gamma(t)},$$

where $\gamma(t)$ is the smooth integral curve realizing $X|_p$ and $Y \subset T\mathcal{M} \subset \mathbb{R}^n$. This is a consequence of [24, Lemma 4.9] specialized to the Euclidean connection, but can also be understood directly from the definition. Note that $Y|_p \in T_p\mathcal{M} \subset T_p\mathbb{R}^n \simeq \mathbb{R}^n$ by the identification $\sum_{i=1}^n v_i \partial_i \leftrightarrow v$ with $v_i \in C^\infty(\mathbb{R}^n)$; see [25, Proposition 3.13].

2.6. The second fundamental form and Weingarten map. For Riemannian embedded submanifolds $\mathcal{M} \subset \mathbb{R}^n$, two Levi–Civita connections are relevant: the connection ∇ for \mathcal{M} and the Euclidean connection $\tilde{\nabla}$ of the ambient \mathbb{R}^n . The Gauss formula [24, Theorem 8.2] relates the two:

$$\tilde{\nabla}_X Y = \nabla_X Y + II(X, Y),$$

where $X, Y \in \mathcal{X}(\mathcal{M})$ and $II(X, Y)$ is the *second fundamental form*. The second fundamental form at p is simply the projection of the ambient covariant derivative onto the normal space $N_p\mathcal{M}$:

$$II_p(X, Y) := (II(X, Y))|_p := P_{N_p\mathcal{M}} \left((\tilde{\nabla}_X Y)|_p \right).$$

Consequently, the covariant derivative $\nabla_X Y$ can also be computed by projecting the ambient Euclidean covariant derivative $\tilde{\nabla}_X Y$ onto the tangent space of \mathcal{M} . The second fundamental form is symmetric in X and Y , so $II_p(X, Y)$ only depends on the tangent vectors $X|_p$ and $Y|_p$, which makes the Gauss formula above well defined; $\tilde{\nabla}_X Y$ actually requires $X, Y \in \mathcal{X}(\mathbb{R}^n)$, but the foregoing remark shows that any smooth extension yields the same result.

The second fundamental form at p is a smooth map $II_p : T_p\mathcal{M} \times T_p\mathcal{M} \rightarrow N_p\mathcal{M}$. Given a normal vector $\eta \in N_p\mathcal{M} \subset \mathbb{R}^n$, the *shape operator* or *Weingarten map* S_η is the symmetric linear map corresponding to the bilinear map

$$H_\eta : T_p\mathcal{M} \times T_p\mathcal{M} \rightarrow \mathbb{R}, (v, w) \mapsto \langle II(v, w), \eta \rangle,$$

where the Euclidean inner product $\langle \cdot, \cdot \rangle$ is the Riemannian metric on \mathbb{R}^n , i.e.,

$$\langle S_\eta(v), w \rangle = H_\eta(v, w) = \langle II(v, w), \eta \rangle.$$

The Weingarten map is a linear map $S_\eta : T_x\mathcal{I} \rightarrow T_x\mathcal{I}$ measuring the difference between the *curvature tensors* of \mathcal{I} and the ambient space \mathbb{R}^n [24, Chapter 8].

An alternative characterization of S_η that we will use to prove Corollary 8 below is given in [14, Section 6.2]:

$$(4) \quad S_\eta : T_p\mathcal{M} \rightarrow T_p\mathcal{M}, v \mapsto P_{T_p\mathcal{M}} \left(-(\tilde{\nabla}_v N)|_p \right),$$

where $P_{T_p\mathcal{M}}$ denotes the orthogonal projection onto $T_p\mathcal{M}$, N is a smooth extension of η to a normal vector field on an open neighborhood of p in \mathcal{M} , and $\tilde{\nabla}_v$ is the Euclidean covariant derivative. In other words, S_η maps η to the tangential part of the usual directional derivative of N in direction of $v \in \mathcal{M} \subset \mathbb{R}^n$. A consequence of [14, Chapter 6, Proposition 2.1] is that the definition of (4) is independent of the choice of extension N , and hence S_η is a well-defined linear map.

Computing the second fundamental form is often facilitated by *pushing forward* vector fields through a diffeomorphism $F : \mathcal{M} \rightarrow \mathcal{N}$. When F is a diffeomorphism, there always exists a vector field Y on \mathcal{N} that is *F-related* to a vector field X on \mathcal{M} : $Y|_p = (F_*X)|_p := (D_{F^{-1}(p)}F)(X|_{F^{-1}(p)})$. The integral curves generated by X and $Y = F_*X$ are related by Proposition 9.6 of [25].

3. THE CONDITION NUMBER OF APPROXIMATION PROBLEMS

We begin by formalizing the computational problem whose condition number we want to study. Conceptually the simplest instance of (IPIP) occurs when the ambient space \mathbb{R}^n is restricted to a tubular neighborhood $\mathcal{T} \subset \mathbb{R}^n$ of \mathcal{I} . If we assume that \mathcal{T} has the property that for each point $a \in \mathcal{T}$ there is a unique point x on \mathcal{I} that minimizes the distance from \mathcal{I} to a , we have the following well-defined computational problem

$$(5) \quad a \mapsto \pi_{\mathcal{O}} \circ \arg \min_{(x,y) \in \mathcal{S}} \frac{1}{2} \|a - \pi_{\mathcal{I}}(x, y)\|^2.$$

Our assumption on \mathcal{T} can always be achieved by suitably restricting the height [21, Chapter 4, Section 5]. The problem in (5) is then called *approximation problem* (AP). For this problem, the implicit formulation is as follows:

$$(AP) \quad \mathcal{S}_{AP} := \{(a, y) \in \mathcal{T} \times \mathcal{O} \mid (P_{\mathcal{I}}(a), y) \in \mathcal{S}\},$$

where $P_{\mathcal{I}} : \mathcal{T} \rightarrow \mathcal{I}, a \mapsto \operatorname{argmin}_{x \in \mathcal{I}} \|x - a\|$ is the nonlinear projection that maps $a \in \mathcal{T}$ to the unique point on \mathcal{I} that minimizes the distance to a .

The condition number of (AP) would then be given by the Shub–Smale framework from (2) to \mathcal{S}_{AP} . However, a priori it is not clear that \mathcal{S}_{AP} has the structure of a smooth submanifold of $\mathcal{T} \times \mathcal{O}$. The essential observation is that it does not need to be! In fact, the definition of the condition number (2) distinguishes well-posed points from ill-posed points, and only for well-posed points the manifold structure is needed.

We define the well-posed tuples for (AP) to be

$$\mathcal{W}_{AP} := \{(a, y) \in \mathcal{T} \times \mathcal{O} \mid (P_{\mathcal{I}}(a), y) \in \mathcal{W}\},$$

and in appendix A.4, we prove the following result (under Assumption 1).

Lemma 1. *\mathcal{W}_{AP} is a smooth embedded submanifold of $\mathcal{T} \times \mathcal{O}$ of dimension n . Moreover, \mathcal{W}_{AP} is dense in \mathcal{S}_{AP} .*

We think this definition is reasonable, because the AP consists of first computing x and then using x as input to compute y . If (x, y) was ill-posed to begin with, the computational problem as a whole should be ill-posed. Moreover, if $\mathcal{W} = \emptyset$ then $\mathcal{W}_{AP} = \emptyset$, so (AP) is ill posed if the original problem is ill posed.

The condition number of the AP is now given by (2). For brevity we drop the subscript of the spectral norm henceforth.

$$(6) \quad \kappa_{AP}(a, y) = \begin{cases} \kappa[\pi_{\mathcal{O}} \circ \pi_{\mathcal{I}}^{-1} \circ P_{\mathcal{I}}](a) & \text{if } (a, y) \in \mathcal{W}_{AP}, \\ \infty & \text{otherwise} \end{cases},$$

where $\pi_{\mathcal{I}}$ and $\pi_{\mathcal{O}}$ are the projections onto the input and output manifolds respectively, and $\pi_{\mathcal{I}}^{-1}$ is the local inverse of $\pi_{\mathcal{I}}$ at $(x, y) \in \mathcal{S}$. Note that $\kappa_{AP}(a, y) < \infty$ for $(a, y) \in \mathcal{W}_{AP}$ by definition, which justifies calling them well-posed tuples. We can now state the first main result, which we prove in appendix A.4.

Theorem 1 (Global minimizer). *Let $a \in \mathcal{T} \subset \mathbb{R}^n$ be sufficiently close to \mathcal{I} , specifically lying in a tubular neighborhood of \mathcal{I} , so that it has a unique closest point $x \in \mathcal{I}$. Let $\eta = a - x$. If $(a, y) \in \mathcal{W}_{AP}$, then*

$$\kappa_{AP}(a, y) = \|(\mathbf{D}_{(x,y)}\pi_{\mathcal{O}})(\mathbf{D}_{(x,y)}\pi_{\mathcal{I}})^{-1}(\mathbf{1} - S_{\eta})^{-1}\|_{\mathcal{I} \rightarrow \mathcal{O}},$$

where $S_{\eta} : \mathbb{T}_x\mathcal{I} \rightarrow \mathbb{T}_x\mathcal{I}$ is the Weingarten map. Moreover, if $(a, y) \in \mathcal{S}_{AP} \setminus \mathcal{W}_{AP}$ then $\mathbf{D}_{(x,y)}\pi_{\mathcal{I}}$ is not invertible.

Corollary 1. *$\kappa_{AP} : \mathcal{S}_{AP} \rightarrow \mathbb{R} \cup \{+\infty\}$ is continuous.*

Remark 1. *If $F : \mathcal{I} \rightarrow \mathcal{O}$ is a smooth map and $\mathcal{S} \subset \mathcal{I} \times \mathcal{O}$ is the graph of F , then the foregoing specializes to $(\mathbf{D}_{(x,F(x))}\pi_{\mathcal{O}})(\mathbf{D}_{(x,F(x))}\pi_{\mathcal{I}})^{-1} = \mathbf{D}_x F$. This observation applies to Theorem 3 as well.*

Curvature has entered the picture in Theorem 1 in the form of the Weingarten map S_{η} . It is an extrinsic property of \mathcal{I} , however, so that the condition number κ_{AP} depends on the Riemannian embedding of \mathcal{I} into some \mathbb{R}^n . Intuitively this is coherent, as different embeddings give rise to different computational problems each with their own sensitivity to perturbations in the ambient space. The contribution of the solution manifold \mathcal{S} to the condition number of the approximation problem, i.e., $(\mathbf{D}_{(x,y)}\pi_{\mathcal{O}})(\mathbf{D}_{(x,y)}\pi_{\mathcal{I}})^{-1}$, is intrinsic and does not depend on the embedding.

The factor involving curvature, i.e., $(\mathbf{1} - S_\eta)^{-1}$, disappears when $S_\eta = 0$. This occurs when the point to approximate lies on the input manifold (so $\eta = 0$). In this case, we have the following result.

Corollary 2. *Let $(x, y) \in \mathcal{S}$. Then, we have $\kappa(x, y) = \kappa_{\text{AP}}(x, y)$.*

Proof. By [34, Theorem 4], $\kappa(x, y) = \|(\mathbf{D}_{(x,y)}\pi_{\mathcal{O}})(\mathbf{D}_{(x,y)}\pi_{\mathcal{I}})^{-1}\|$. Comparing with Theorem 1 proves the assertion. \square

In other words, if the input data is exactly on \mathcal{I} , the condition number of (AP) equals the condition number of the computational problem \mathcal{S} . By continuity, the effect of curvature on the sensitivity of the computational problem can essentially be ignored for small $\|\eta\|$, i.e., for points very close to \mathcal{I} . This is convenient in practice because computing the Weingarten map is often substantially more complicated than obtaining the derivatives of the projection maps $\pi_{\mathcal{O}}$ and $\pi_{\mathcal{I}}$.

4. THE CONDITION NUMBER OF CRITICAL POINT PROBLEMS

The projection $\mathbf{P}_{\mathcal{I}}$ onto the input manifold \mathcal{I} often has no closed-form expression for nonlinear manifolds. Therefore, in applications involving the problem (AP), the projection is often approximated via some optimization procedure applied to a distance function, as in the example in Section 8. For nonconvex manifolds \mathcal{I} , optimization methods usually only guarantee that the first-order optimality conditions are satisfied [2]. This made us wonder about the condition number of (AP) where we replace the projection $\mathbf{P}_{\mathcal{I}}$ by a map that produces one of the points satisfying these first-order optimality conditions, further generalizing the (AP) to a computational problem that we call the *generalized critical point problem* (GCPP). This most general formulation is discussed in the next section. Here, we first study a special case that is important to understand the general case.

The special case arises when the solution manifold $\mathcal{S} \subset \mathcal{I} \times \mathcal{O}$ is the graph of the identity map $\mathbf{1} : \mathcal{I} \rightarrow \mathcal{I}$, so $\mathcal{O} = \mathcal{I}$. Given a point $a \in \mathbb{R}^n$, the problem in (AP) comprises finding an output $x \in \mathcal{I}$ so that $\|x - a\|$ is minimized in the Euclidean distance. This is a textbook example of a Riemannian optimization problem. Indeed, it can be formulated as the least-squares problem

$$(7) \quad \min_{x \in \mathcal{I}} \frac{1}{2} \|a - x\|^2 = \mathbf{P}_{\mathcal{I}}(a).$$

Computing *global* minimizers of this optimization problem is usually too ambitious a task when \mathcal{I} is a complicated nonlinear and nonconvex manifold. Most Riemannian optimization methods will therefore only seek to satisfy the first-order necessary optimality conditions of (7), namely $a - x \in \mathbf{N}_x\mathcal{I}$. We say that such optimization methods attempt to solve the *critical point problem* (CPP). In general, the implicit formulation of the CPP is as follows:

$$(CPP) \quad \mathcal{S}_{\text{CPP}} := \{(a, x) \in \mathbb{R}^n \times \mathcal{I} \mid x - a \in \mathbf{N}_x\mathcal{I}\}.$$

We call \mathcal{S}_{CPP} the *critical point locus* and have the following result.

Lemma 2. *\mathcal{S}_{CPP} is an embedded submanifold of $\mathbb{R}^n \times \mathcal{I}$ of dimension n .*

Consequently, the CPP falls into the realm of the theory of condition from (2). For distinguishing them from the projections associated to \mathcal{S} , we denote the coordinate projections of \mathcal{S}_{CPP} by $\Pi_{\mathbb{R}^n} : \mathcal{S}_{\text{CPP}} \rightarrow \mathbb{R}^n$ and $\Pi_{\mathcal{I}} : \mathcal{S}_{\text{CPP}} \rightarrow \mathcal{I}$. The corresponding submanifold of well-posed tuples is

$$\mathcal{W}_{\text{CPP}} := \{(a, x) \in \mathbb{R}^n \times \mathcal{I} \mid \mathbf{D}_{(a,x)}\Pi_{\mathbb{R}^n} \text{ is invertible}\}.$$

The fact that it is a manifold is the following result, proved in appendix A.1.

Lemma 3. *\mathcal{W}_{CPP} is an open dense embedded submanifold of \mathcal{S}_{CPP} .*

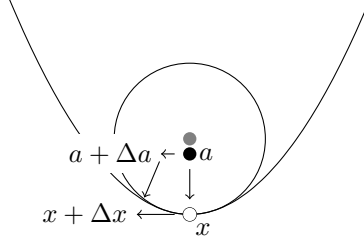


FIGURE 1. The graph shows an input a for the CPP of the parabola. The circle with critical radius is above the parabola, its center (the gray point) is a focal point of the parabola, i.e., it is a point in $\Sigma_{\text{CPP}} = \mathcal{S}_{\text{CPP}} \setminus \mathcal{W}_{\text{CPP}}$. The point a also lies above the parabola, so $\eta = a - x$ points towards the focal point. This means that the principal curvature at x in direction of η is $c_1 > 0$. Moreover, $c_1 \|\eta\| < 1$, and thus, by (8), we have $\kappa_{\text{CPP}}(a, x) > 1$. In other words, the curvature of the parabola amplifies the perturbation $\|\Delta a\|$.

The condition number associated to (CPP) is

$$\kappa_{\text{CPP}}(a, x) = \begin{cases} \kappa[\Pi_{\mathcal{I}} \circ \Pi_{\mathbb{R}^n}^{-1}](a), & \text{if } (a, x) \in \mathcal{W}_{\text{CPP}}, \\ \infty & \text{otherwise,} \end{cases}$$

and $\Pi_{\mathbb{R}^n}^{-1}$ is the local inverse of $\Pi_{\mathbb{R}^n}$ at $(a, x) \in \mathcal{W}_{\text{CPP}}$. As the next theorem shows, the condition number of the CPP depends on the curvature of \mathcal{I} and the distance from a to x . This second main result is proved in appendix A.1.

Theorem 2 (Critical points). *Let $(a, x) \in \mathcal{W}_{\text{CPP}}$ and $\eta := a - x$. Then,*

$$\kappa_{\text{CPP}}(a, x) = \|(\mathbf{1} - S_\eta)^{-1}\|_{\mathcal{I} \rightarrow \mathcal{I}},$$

where $S_\eta : T_x \mathcal{I} \rightarrow T_x \mathcal{I}$ is the Weingarten map. Moreover, if $(a, x) \in \mathcal{S}_{\text{CPP}} \setminus \mathcal{W}_{\text{CPP}}$, then $\mathbf{1} - S_\eta$ is not invertible.

Corollary 3. $\kappa_{\text{CPP}} : \mathcal{S}_{\text{CPP}} \rightarrow \mathbb{R} \cup \{+\infty\}$ is continuous.

Let us investigate the meaning of this theorem a little further. For $\eta \neq 0$, let $w := \frac{\eta}{\|\eta\|}$ and let c_1, \dots, c_m be the eigenvalues of $S_w = \frac{1}{\|\eta\|} S_\eta$. The map S_η is self-adjoint, so that the c_i are all real. The eigenvalues of S_η are then $c_1 \|\eta\|, \dots, c_m \|\eta\|$, so that Theorem 2 implies that

$$(8) \quad \kappa_{\text{CPP}}(a, x) = \max_{1 \leq i \leq m} \frac{1}{|1 - c_i \|\eta\||}, \text{ where } \eta = a - x.$$

In particular, if $\|\eta\|c_i = 1$ for some i , then $\kappa_{\text{CPP}}(a, x) = \infty$. The c_i are called *principal curvatures* of \mathcal{I} at x in direction of η , and they have the following classic geometric meaning [40, Chapter 1]. If $u_i \in T_x \mathcal{I}$ is a unit length eigenvector of the eigenvalue c_i , then locally around x and in the direction of u_i the manifold \mathcal{I} contains an infinitesimal arc of a circle with center $x + c_1^{-1} w = x + (c_i \|\eta\|)^{-1} \eta$ containing x . This circle is called an *osculating circle*. The radii $r_1 := |c_1|^{-1}, \dots, r_m := |c_m|^{-1}$ of those circles are called the *critical radii* of \mathcal{I} at x in direction η . Consequently, $\kappa_{\text{CPP}}(a, x) = \infty$ if and only if \mathcal{I} contains an infinitesimal arc of the circle with center $x + \eta = a$. In other words, if $\|\eta\|$ lies close to any of the critical radii then the CPP is ill-conditioned at (a, x) .

The formula from (8) makes it apparent that for some inputs we may have that $\kappa_{\text{CPP}}(a, x) < 1$. In other words, for some input points $a \in \mathbb{R}^n$ the infinitesimal

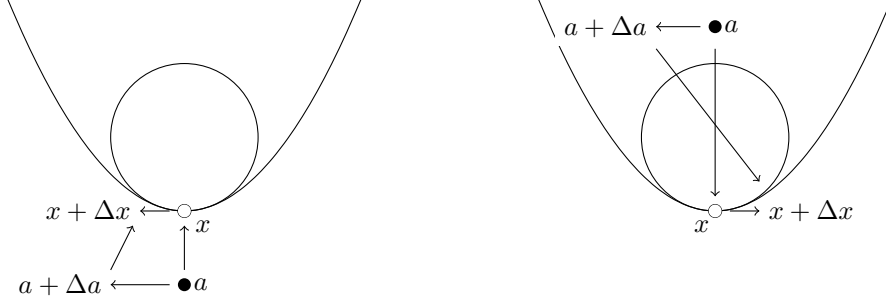


FIGURE 2. The picture shows two inputs for the critical point problem of the parabola other than in Figure 1. In the left picture the point a lies below the parabola, so $\eta = a - x$ points away from the focal point. This means that the principal curvature at x in direction of η is $c_1 < 0$, so that by (8) we have $\kappa_{\text{CPP}}(a, x) < 1$. The curvature of the parabola shrinks the perturbation $\|\Delta a\|$. The right picture shows a point a , which lies above the parabola, so that the corresponding critical curvature is positive. However, $c_1\|\eta\| > 1$, and so by (8) we have $\kappa_{\text{CPP}}(a, x) < 1$. Again, the curvature of the parabola shrinks the perturbation $\|\Delta a\|$.

error $\|\Delta a\|$ can shrink! Figure 1 and 2 give a geometric explanation of when the error is shrunk and when it is amplified.

We also have an interpretation of $\kappa_{\text{CPP}}(a, x)$ as a normalized inverse distance to ill-posedness: for $(a, x) \in \mathcal{S}_{\text{CPP}}$, let $\eta = a - x$ be the normal vector that connects x to a . The locus of ill-posed inputs for the CPP is $\Sigma_{\text{CPP}} = \mathcal{S}_{\text{CPP}} \setminus \mathcal{W}_{\text{CPP}}$. The projection $\Pi_{\mathbb{R}^n}(\Sigma_{\text{CPP}})$ is well studied in the literature. Thom [43] calls it the *target envelope*¹ of \mathcal{S}_{CPP} , while Porteous [33] calls it the *focal set* of \mathcal{I} , and for curves in the plane it is called the *evolute*; see Chapter 10 of [30]. The points in the intersection $\{x\} \times (x + \mathbb{R}\eta)$ with Σ_{CPP} are given by the multiples of the normal vector η whose length equals one of the critical radii r_1, \dots, r_m ; this is also visible in Figure 5. Comparing with (8) we find

$$\frac{1}{\kappa_{\text{CPP}}(a, x)} = \min_{\eta_0 \in \mathbb{R}\eta: (x, a + \eta_0) \in \Sigma_{\text{CPP}}} \frac{\|\eta_0\|}{\left| \|\eta_0\| - \|\eta\| \right|}, \text{ where } \eta = a - x.$$

This interpretation of the condition number is in the spirit of Demmel [12, 13].

Remark 2. *If \mathcal{I} is a smooth algebraic variety in \mathbb{R}^n , then solving \mathcal{S}_{CPP} reduces to solving a system of polynomial equations. For almost all inputs $a \in \mathbb{R}^n$ this system has a constant number of solutions over the complex numbers, called the Euclidean distance degree [15]. Theorem 2 thus characterizes the condition number of real solutions of this special system of polynomial equations.*

5. THE CONDITION NUMBER OF GENERAL CRITICAL POINT PROBLEMS

Having studied the special case of projecting a point in the ambient space \mathbb{R}^n to a critical point of the distance to \mathcal{I} , we are now ready to consider the most general formulation that we treat in this work. As mentioned before, our motivation stems from solving (AP) when a closed-form solution of the projection $P_{\mathcal{I}}$ is lacking. Using Riemannian optimization methods for solving problem (7), one can in general only hope to find points satisfying the first-order optimality conditions [2], as with

¹Actually, Thom calls it the target envelope of the normal bundle of \mathcal{I} . However, as shown in the proof of Lemma 2, the normal bundle of \mathcal{I} is diffeomorphic to \mathcal{S}_{CPP} .

Riemannian Gauss–Newton methods.² This results in a *generalized critical point problem*: given $a \in \mathbb{R}^n$, produce an output $y \in \mathcal{O}$ such that there is a corresponding $x \in \mathcal{I}$ that satisfies the first-order optimality conditions of (7). We can implicitly formulate this computational problem as follows:

$$(\text{GCPP}) \quad \mathcal{S}_{\text{GCPP}} := \{(a, x, y) \in \mathbb{R}^n \times \mathcal{I} \times \mathcal{O} \mid (a, x) \in \mathcal{S}_{\text{CPP}} \text{ and } (x, y) \in \mathcal{S}\}.$$

The solution manifold $\mathcal{S}_{\text{GCPP}}$ is defined using three factors: the first is the input and the third is the output. The second factor \mathcal{I} encodes how the output is obtained from the input. We believe it is reasonable to label those triples ill-posed where either $(x, y) \in \mathcal{S}$ is ill-posed for the original problem or $(a, x) \in \mathcal{S}_{\text{CPP}}$ is ill-posed for the (CPP). Therefore, the well-posed locus is

$$\mathcal{W}_{\text{GCPP}} := \{(a, x, y) \in \mathbb{R}^n \times \mathcal{I} \times \mathcal{O} \mid (a, x) \in \mathcal{W}_{\text{CPP}} \text{ and } (x, y) \in \mathcal{W}\}.$$

As before, it is not important if $\mathcal{S}_{\text{GCPP}}$ is a manifold, because it is sufficient that the well-posed tuples form a manifold. We prove this in appendix A.2.

Lemma 4. $\mathcal{W}_{\text{GCPP}}$ is an embedded submanifold of $\mathbb{R}^n \times \mathcal{W}$ of dimension n . Moreover, $\mathcal{W}_{\text{GCPP}}$ is dense in $\mathcal{S}_{\text{GCPP}}$.

Consequently, we can use the definition of condition from (2). We denote by $\Pi_{\mathbb{R}^n} : \mathcal{W}_{\text{GCPP}} \rightarrow \mathbb{R}^n$ and $\Pi_{\mathcal{O}} : \mathcal{W}_{\text{GCPP}} \rightarrow \mathcal{O}$ the projection onto the first and third factor of $\mathcal{W}_{\text{GCPP}}$, respectively.³ The condition number of the GCPP is then

$$(9) \quad \kappa_{\text{GCPP}}(a, x, y) = \begin{cases} \kappa[\Pi_{\mathcal{O}} \circ \Pi_{\mathbb{R}^n}^{-1}](a) & \text{if } (a, x, y) \in \mathcal{W}_{\text{GCPP}}, \\ \infty & \text{otherwise,} \end{cases}$$

where $\Pi_{\mathbb{R}^n}^{-1}$ is a local inverse of $\Pi_{\mathbb{R}^n}$ at $(a, x, y) \in \mathcal{W}_{\text{GCPP}}$. As above for the approximation problem, we have $\kappa_{\text{GCPP}}(a, x, y) < \infty$ for tuples $(a, x, y) \in \mathcal{W}_{\text{GCPP}}$, which justifies calling those tuples well-posed. Our final main result generalizes Theorem 1; it is proved in appendix A.2.

Theorem 3 (Generalized critical points). *Let $(a, x, y) \in \mathcal{W}_{\text{GCPP}}$ and let $\eta = a - x$. Then, we have*

$$\kappa_{\text{GCPP}}(a, x, y) = \|(\mathbf{D}_{(x,y)}\pi_{\mathcal{O}})(\mathbf{D}_{(x,y)}\pi_{\mathcal{I}})^{-1}(\mathbf{1} - S_{\eta})^{-1}\|_{\mathcal{I} \rightarrow \mathcal{O}},$$

where $\pi_{\mathcal{I}} : \mathcal{S} \rightarrow \mathcal{I}$ and $\pi_{\mathcal{O}} : \mathcal{S} \rightarrow \mathcal{O}$ are coordinate projections of \mathcal{S} , and $S_{\eta} : T_x\mathcal{I} \rightarrow T_x\mathcal{I}$ is the Weingarten map in the direction η . Moreover, if $(a, x, y) \in \mathcal{S}_{\text{GCPP}} \setminus \mathcal{W}_{\text{GCPP}}$, then either $\mathbf{D}_{(x,y)}\pi_{\mathcal{I}}$ or $\mathbf{1} - S_{\eta}$ is not invertible.

Corollary 4. $\kappa_{\text{GCPP}} : \mathcal{S}_{\text{GCPP}} \rightarrow \mathbb{R} \cup \{+\infty\}$ is continuous.

An immediate corollary from this theorem is obtained by using (8) and the submultiplicativity of the spectral norm.

Corollary 5. *Let $(a, x, y) \in \mathcal{S}_{\text{GCPP}}$ and $\eta = a - x$. We have*

$$\frac{\kappa(x, y)}{\max_{1 \leq i \leq m} |1 - c_i \|\eta\|} \leq \kappa_{\text{GCPP}}(a, x, y) \leq \frac{\kappa(x, y)}{\min_{1 \leq i \leq m} |1 - c_i \|\eta\|},$$

where c_1, \dots, c_m are the principal curvatures of \mathcal{I} at x in direction η , and $\kappa(x, y)$ is the condition number of the computational problem modeled by \mathcal{S} .

Proof. By [34, Theorem 4], $\kappa(x, y) = \|(\mathbf{D}_{(x,y)}\pi_{\mathcal{O}})(\mathbf{D}_{(x,y)}\pi_{\mathcal{I}})^{-1}\|$. The submultiplicativity of the spectral norm yields $\kappa(x, y) \leq \kappa_{\text{GCPP}}(a, x, y)\|\mathbf{1} - S_{\eta}\|$ and $\kappa_{\text{GCPP}}(a, x, y) \leq \kappa(x, y)\|(\mathbf{1} - S_{\eta})^{-1}\|$. The $c_i \|\eta\|$, $1 \leq i \leq m$, are the eigenvalues of the symmetric operator S_{η} . The proof is concluded. \square \square

²In [7] we analyzed the connection between the condition number and convergence properties of RGN methods for solving (PIP).

³We are using the same notation as for \mathcal{W}_{CPP} , but this should not cause confusion as the latter is a special case of the GCPP.

6. IMPLICATIONS FOR RIEMANNIAN OPTIMIZATION

In Section 4, we established a connection between the CPP and the Riemannian optimization problem (7): \mathcal{S}_{CPP} is the manifold of *critical tuples* $(a, x) \in \mathbb{R}^n \times \mathcal{I}$, such that x is a critical point of the squared distance function from \mathcal{I} to a . For the general implicit formulations in (AP) and (GCPP), however, the connection to Riemannian optimization is perhaps not completely evident. The motivation for considering (AP) and (GCPP) was that Riemannian optimization methods only guarantee to satisfy (numerically) the necessary first-order optimality conditions [2]. However, in the most general situation the solution manifold \mathcal{S} is such that there are several outputs $y \in \mathcal{O}$ for an input \mathcal{I} . In this case we must treat all those tuples $(x, y) \in \mathcal{S}$ separately. This is the reason for the restriction to open neighborhoods in the following proposition.

An important special case arises when \mathcal{S} is the graph of a *local diffeomorphism* $F : \mathcal{O} \rightarrow \mathcal{I}$. Proposition 1 below establishes the connection between the solutions of (AP) and the global minimizers of the Riemannian optimization problem $\min_{y \in \mathcal{O}} \frac{1}{2} \|a - F(y)\|^2$ from (PIP) in this case.

Proposition 1. *Let the input manifold \mathcal{I} , output manifold \mathcal{O} , well-posed loci \mathcal{W} and \mathcal{W}_{AP} be as in (AP). Assume that $(a^*, y^*) \in \mathcal{W}_{\text{AP}}$ is a well-posed tuple for the (AP) with $x^* \in \mathcal{I}$ the point closest to a^* . Then, there exists an open neighborhood $\mathcal{N}_{(x^*, y^*)} \subset \mathcal{W}$ of (x^*, y^*) and a tubular neighborhood $\mathcal{T}_{a^*} \subset \mathcal{T}$ of $\pi_{\mathcal{I}}(\mathcal{N}_{(x^*, y^*)})$, which contains a^* , so that the Riemannian optimization problem*

$$\rho_{(a^*, y^*)} : \mathcal{T}_{a^*} \rightarrow \mathcal{O}, \quad a \mapsto \pi_{\mathcal{O}} \circ \underset{(x, y) \in \mathcal{N}_{(x^*, y^*)}}{\operatorname{argmin}} \frac{1}{2} \|a - \pi_{\mathcal{I}}(x, y)\|^2$$

is an instance of (AP) and its condition number at (a, y) is $\kappa_{\text{AP}}(a, y)$.

The solutions of the GCPP were defined as the generalization of the AP to critical points. However, we did not show that they too can be seen as the critical tuples of a distance function optimized over in a Riemannian optimization problem. This connection is established next and proved in appendix A.3.

Proposition 2. *$(a, x, y) \in \mathcal{W}_{\text{GCPP}}$ if and only if $(a, (x, y))$ is a well-posed critical tuple of the function optimized over in the Riemannian optimization problem*

$$\min_{(x, y) \in \mathcal{W}} \frac{1}{2} \|a - \pi_{\mathcal{I}}(x, y)\|^2.$$

Our main motivation for studying critical points instead of only the global minimizer as in (AP) stems from our desire to predict the sensitivity of outputs of Riemannian optimization methods for solving approximation problems like (7) and (PIP). When applied to a well-posed optimization problem, these methods in general only guarantee convergence to critical points [2]. However, in practice, convergence to critical points that are not local minimizers is extremely unlikely [2]. The reason is that they are *unstable outputs* of these algorithms: Applying a tiny perturbation to such critical points will cause the optimization method to escape their vicinity, and with high probability, converge to a local minimizer instead.

Remark 3. *One should be careful to separate condition from stability. The former is a property of a problem, the latter the property of an algorithm. We do not claim that computing critical points of GCPPs other than local minimizers are ill-conditioned problems. We only claim that many Riemannian optimization methods are unstable algorithms for computing them. This is not a bad property, since the goal in Riemannian optimization is to find minimizers, not critical points!*

For critical points of the GCPP that are local minimizers, it is reasonable to expect that we can connect their condition number to a Riemannian optimization

problem like (AP). The next result shows that such a correspondence is obtained by restricting the GCPP to a neighborhood of the local minimizer.

Theorem 4 (Condition of local minimizers). *Let the input manifold \mathcal{I} , the output manifold \mathcal{O} , and well-posed loci \mathcal{W} and $\mathcal{W}_{\text{GCPP}}$ be as in (GCPP). Assume that $(a^*, x^*, y^*) \in \mathcal{W}_{\text{GCPP}}$ and x^* is a local minimizer of $d_{a^*} : \mathcal{I} \rightarrow \mathbb{R}, x \mapsto \frac{1}{2}\|a^* - x\|^2$. Then, there exist open neighborhoods $\mathcal{A}_{a^*} \subset \mathbb{R}^n$ around a^* and $\mathcal{N}_{(x^*, y^*)} \subset \mathcal{W}$ around (x^*, y^*) , so that the Riemannian optimization problem*

$$\rho_{(a^*, x^*, y^*)} : \mathcal{A}_{a^*} \rightarrow \mathcal{O}, \quad a \mapsto \pi_{\mathcal{O}} \circ \underset{(x, y) \in \mathcal{N}_{(x^*, y^*)}}{\operatorname{argmin}} \frac{1}{2}\|a - \pi_{\mathcal{I}}(x, y)\|^2$$

is an (AP) and its condition number is $\kappa_{\text{GCPP}}(a, x, y) = \kappa_{\text{AP}}(a, y)$.

Taking $\mathcal{I} = \mathcal{O}$ and \mathcal{S} as the graph of the identity map $\mathbf{1}$, the following result is immediate.

Corollary 6. *Let the input manifold \mathcal{I} , and well-posed loci \mathcal{W} and \mathcal{W}_{CPP} be as in (CPP). Assume that $(a^*, x^*) \in \mathcal{W}_{\text{CPP}}$ is well-posed and that x^* is a local minimizer of $d_{a^*} : \mathcal{I} \rightarrow \mathbb{R}, x \mapsto \frac{1}{2}\|a^* - x\|^2$. Then, there exist open neighborhoods $\mathcal{A}_{a^*} \subset \mathbb{R}^n$ around a^* and $\mathcal{I}_{x^*} \subset \mathcal{I}$ around x^* , so that the Riemannian optimization problem*

$$\rho_{(a^*, x^*)} : \mathcal{A}_{a^*} \rightarrow \mathcal{I}, \quad a \mapsto \underset{x \in \mathcal{I}_{x^*}}{\operatorname{argmin}} \frac{1}{2}\|a - x\|^2$$

is an (AP) and its condition number at (a, x) is $\kappa_{\text{CPP}}(a, x) = \kappa_{\text{AP}}(a, x)$.

7. CAPTURING CURVATURE WITH THE WEINGARTEN MAP

Having presented the main results involving the three computational problems (AP, CPP, GCPP) and their condition numbers, we now explain how the Weingarten map appears in all of them. A common theme in all three problems is that they involve a projection, $\Pi_{\mathcal{I}} : \mathcal{N}\mathcal{I} \rightarrow \mathcal{I}, (x, \eta) \mapsto x$, from the normal bundle $\mathcal{N}\mathcal{I}$ to the base of the bundle, \mathcal{I} , as first step. Indeed, the first step in the AP, applying $P_{\mathcal{I}}$, can be interpreted as projecting a point $a \in \mathbb{R}^n$ to the closest critical point $x \in \mathcal{I}$ of the distance function. There is a unique normal vector $\eta \in \mathcal{N}_x\mathcal{I}$ such that $a = x + \eta$, so a can be identified with $(x, \eta) \in \mathcal{N}\mathcal{I}$. The CPP, on the other hand, projects the ambient a to one particular critical point, determined implicitly by \mathcal{S}_{CPP} . By definition $(a, x) \in \mathcal{S}_{\text{CPP}}$ if $\eta := a - x \in \mathcal{N}_x\mathcal{I}$, so there is an identification of (a, x) with $(x, \eta) \in \mathcal{N}\mathcal{I}$. Finally, the GCPP consists of the CPP composed with an implicitly given map from \mathcal{I} to \mathcal{O} .

The projection $\Pi_{\mathcal{I}}$ is a smooth map [25, Corollary 10.36]. Since all foregoing computational problems, under suitable identifications, can be interpreted as composing another map with $\Pi_{\mathcal{I}}$, we can anticipate that its derivative contributes to the condition number. This derivative

$$D_{(x, \eta)}\Pi_{\mathcal{I}} : T_{(x, \eta)}\mathcal{N}\mathcal{I} \rightarrow T_x\mathcal{I}$$

is characterized in the next theorem for embedded submanifolds $\mathcal{I} \subset \mathbb{R}^n$.

Theorem 5. *Let $(x, \eta) \in \mathcal{N}\mathcal{I}$ be in the normal bundle and $(\dot{x}, \dot{\eta}) \in T_{(x, \eta)}\mathcal{N}\mathcal{I}$. Then, $P_{T_x\mathcal{I}}(\dot{x} + \dot{\eta}) = (\mathbf{1} - S_{\eta})\dot{x}$, where $S_{\eta} : T_x\mathcal{I} \rightarrow T_x\mathcal{I}$ is the Weingarten map at x in direction η .*

Corollary 7. *Let $(a, x) \in \mathcal{S}_{\text{CPP}} \subset \mathbb{R}^n \times \mathcal{I}$ and $(\dot{a}, \dot{x}) \in T_{(a, x)}\mathcal{S}_{\text{CPP}}$. Then,*

$$P_{T_x\mathcal{I}}(\dot{a}) = (\mathbf{1} - S_{\eta})\dot{x},$$

where $\eta = a - x$, and $S_{\eta} : T_x\mathcal{I} \rightarrow T_x\mathcal{I}$ is the Weingarten map at x in the direction of η .

The above theorem and corollary are two equivalent formulations. It suffices to prove only one of the two. The proof strategy we employ dates back at least to Weyl [46], whose argument we applied in modern terminology.

Proof of Theorem 5. We can write $a = x + \eta$ with $x \in \mathcal{M}$ and $\eta \in N_x\mathcal{M}$. Let N_1, \dots, N_{n-m} be a local smooth frame of the normal bundle of the m -dimensional embedded manifold $\mathcal{M} \subset \mathbb{R}^n$ near x . A smooth extension of η to the normal bundle of \mathcal{M} is then $N := \sum_{i=1}^{n-m} \alpha_i N_i$, where the $\alpha_i \in \mathbb{R}$ are the coefficients such that $\eta = \sum_{i=1}^{n-m} \alpha_i N_i|_x$. Take a smooth curve $x(t) \in \mathcal{M}$ with $x(0) = x$ and velocity $\frac{d}{dt}x(t)|_{t=0} = \dot{x} \in T_x\mathcal{M}$. Then, we construct the following curve in \mathbb{R}^n : $a(t) = x(t) + \eta(t) = x(t) + \sum_{i=1}^{n-m} \alpha_i N_i|_{x(t)}$. Note that this expression is well-formed, as $N_i|_{x(t)} \in N_{x(t)}\mathcal{M} \subset T_{x(t)}\mathbb{R}^n \simeq \mathbb{R}^n$. Taking derivatives at $t = 0$, we find

$$\dot{a} = \frac{d}{dt}a(t) = \dot{x} + \sum_{i=1}^{m-n} \alpha_i (\tilde{\nabla}_{\dot{x}} N_i)|_x = \dot{x} + (\tilde{\nabla}_{\dot{x}} N)|_x,$$

where the second equality is by definition of the Euclidean connection and the last equality is due to the linearity of the connection. Projecting both sides to the tangent space $T_x\mathcal{M}$ yields

$$P_{T_x\mathcal{M}}(\dot{a}) = \dot{x} + P_{T_x\mathcal{M}}\left((\tilde{\nabla}_{\dot{x}} N)|_x\right) = \dot{x} - S_\eta \dot{x} = (\mathbf{1} - S_\eta)\dot{x},$$

where we used (4) in the second step. \square \square

A useful consequence of the foregoing results is that it allows us to characterize when $\mathbf{1} - S_\eta$ is singular.

Lemma 5. *Let $(a, x) \in \mathcal{S}_{\text{CPP}}$, $\eta = a - x$, and $S_\eta : T_x\mathcal{I} \rightarrow T_x\mathcal{I}$ be the Weingarten map at x in direction η . Then, $\mathbf{1} - S_\eta$ is invertible if and only if $(a, x) \in \mathcal{W}_{\text{CPP}}$.*

Proof. Let $(\dot{a}, \dot{x}) \in T_{(a,x)}\mathcal{S}_{\text{CPP}}$. Then, we have $\dot{x} = (D_{(a,x)}\Pi_{\mathcal{I}})(\dot{a}, \dot{x})$ and $\dot{a} = (D_{(a,x)}\Pi_{\mathbb{R}^n})(\dot{a}, \dot{x})$, so that Corollary 7 yields the equality of operators

$$(10) \quad P_{T_x\mathcal{I}} D_{(a,x)}\Pi_{\mathbb{R}^n} = (\mathbf{1} - S_\eta) D_{(a,x)}\Pi_{\mathcal{I}}.$$

On the one hand, if $(a, x) \in \mathcal{W}_{\text{CPP}}$ then the map $D_{(a,x)}\Pi_{\mathbb{R}^n}$ is invertible. By multiplying with its inverse we get $P_{T_x\mathcal{I}} = (\mathbf{1} - S_\eta)(D_{(a,x)}\Pi_{\mathcal{I}})(D_{(a,x)}\Pi_{\mathbb{R}^n})^{-1}$. As $\mathbf{1} - S_\eta$ is an endomorphism on $T_x\mathcal{I}$, which is the range of the left-hand side, the equality requires $\mathbf{1} - S_\eta$ to be an automorphism, i.e., it is invertible.

On the other hand, if $(a, x) \notin \mathcal{W}_{\text{CPP}}$, there is some $(\dot{a}, \dot{x}) \neq 0$ in the kernel of $D_{(a,x)}\Pi_{\mathbb{R}^n}$. Since $\dot{a} = (D_{(a,x)}\Pi_{\mathbb{R}^n})(\dot{a}, \dot{x}) = 0$, we must have $\dot{x} \neq 0$. Consequently, applying both sides of (10) to (\dot{a}, \dot{x}) gives $0 = (\mathbf{1} - S_\eta)\dot{x}$, which implies that $\mathbf{1} - S_\eta$ is singular. This finishes the proof. \square \square

The next result follows almost directly from Theorem 5. The earliest statement we could locate is due to Abatzoglou [1, Theorem 4.1], who presented it for C^2 embedded submanifolds of \mathbb{R}^n and in a local coordinate chart without reference to the second fundamental form or Weingarten map. Another formulation in a local coordinate chart appears in [16, Lemma 4.1]. A more modern formulation is due to Ambrosio and Mantegazza [4, Theorem 3.8]. Recently it was rediscovered in [26, Theorem C]. The special case of points on the manifold has also been rediscovered several times, for example in [3, Lemma 4].

Corollary 8. *Let $\mathcal{M} \subset \mathbb{R}^n$ be a Riemannian embedded submanifold of dimension m . Then, there exists a tubular neighborhood \mathcal{T} of \mathcal{M} such that the projection map $P_{\mathcal{M}} : \mathcal{T} \rightarrow \mathcal{M}, a \mapsto \min_{x \in \mathcal{M}} \|a - x\|^2$ is a smooth submersion with derivative*

$$D_a P_{\mathcal{M}} = (\mathbf{1} - S_\eta)^{-1} P_{T_x\mathcal{M}},$$

where $x = P_{\mathcal{M}}(a)$, $\eta = a - x$, and $S_{\eta} : T_x\mathcal{M} \rightarrow T_x\mathcal{M}$ is the Weingarten map in the direction of η .

Proof. There exists a tubular neighborhood \mathcal{T} such that the projection to the base of the bundle is the projection map $P_{\mathcal{M}}$ by [21, Chapter 4, Section 5]. Then, the first part about the submersion follows from the definition of a tubular neighborhood; see [25, Proposition 6.25].

The projection map $P_{\mathcal{M}}$ is equivalent to the map that takes a point to the closest critical point of the squared distance to the manifold \mathcal{M} . By definition of \mathcal{T} , the closest critical point of $(x, \eta) \in \mathcal{T} \subset N\mathcal{M}$ is the base $x \in \mathcal{M}$. Therefore, restricted to \mathcal{T} , $P_{\mathcal{M}}|_{\mathcal{T}} = \Pi_{\mathcal{M}}$, where the latter is the projection to the base of the bundle. Since it is a submersion, $(a, x) \in \mathcal{T}$ also lives in \mathcal{W}_{CPP} . The result follows from Lemma 5 and (10). \square \square

8. TRIANGULATION IN COMPUTER VISION

A rich source of approximation problems whose condition can be studied with the proposed framework is multiview geometry in computer vision; for an introduction to this domain see [17, 18, 29]. The tasks consist of recovering information from $r \geq 2$ camera projections of a scene in the world \mathbb{R}^3 . We consider the *pinhole camera model*. In this model the image formation process is modeled by the following transformation, as visualised in Figure 3.

$$\mu_r : y \mapsto \left[\frac{A_{\ell}y + b_{\ell}}{c_{\ell}^T y + d_{\ell}} \right]_{\ell=1}^r,$$

where $A_{\ell} \in \mathbb{R}^{2 \times 3}$, $b_{\ell} \in \mathbb{R}^2$, $c_{\ell} \in \mathbb{R}^3$, and $d_{\ell} \in \mathbb{R}$; see [17, 18, 29]. Clearly, μ_r is not defined on all of \mathbb{R}^3 . We clarify its domain in Lemma 6 below.

A list of points $x = \mu_r(y) \in \mathbb{R}^{2r}$ obtained by this image formation process is called a *consistent point correspondence*. Information that can often be uniquely identified from several consistent point correspondences include the camera parameters and scene structure [17, 18, 29].

As an example application of our theory we compute the condition number of the *triangulation problem* in computer vision [18, Chapter 12]. In this computational problem we are given $r \geq 2$ stationary projective cameras and a consistent point correspondence $x = (x_1, x_2, \dots, x_r) \in \mathbb{R}^{2r}$. The goal is to retrieve the world point $y \in \mathbb{R}^3$ from which they originate. Since the imaging process is subject to noisy measurements and the above idealized projective camera model holds only approximately [18], we expect that instead of x we are given a list $a = (a_1, a_2, \dots, a_r)$ close to x . Thus, x is the true input of the computational problem, y is the output and a is the noisy input.

According to [18, p. 314], the “gold standard algorithm” for triangulation solves the (Riemannian) optimization problem

$$(11) \quad \min_{y \in \mathbb{R}^3} \frac{1}{2} \|a - \mu_r(y)\|^2.$$

From this description we learn that the triangulation computational problem can be cast as a GCCP provided that two conditions hold: (i) the set of consistent point correspondences is an embedded manifold, and (ii) intersecting the back-projected rays is a smooth map from aforementioned manifold to \mathbb{R}^3 . We verify both conditions in the following subsection.

8.1. The multiview manifold. The image formation process can be interpreted as a projective transformation from the projective space \mathbb{P}^3 to \mathbb{P}^2 in terms of the 4×3 camera matrices $P_{\ell} = \begin{bmatrix} A_{\ell} & b_{\ell} \\ c_{\ell}^T & d_{\ell} \end{bmatrix}$. It yields homogeneous coordinates of $x_{\ell} = (z_1^{\ell}/z_3^{\ell}, z_2^{\ell}/z_3^{\ell}) \in \mathbb{R}^2$ where $z^{\ell} = P_{\ell} \begin{bmatrix} y \\ 1 \end{bmatrix}$. Note that if $z_3^{\ell} = 0$ then the point y has

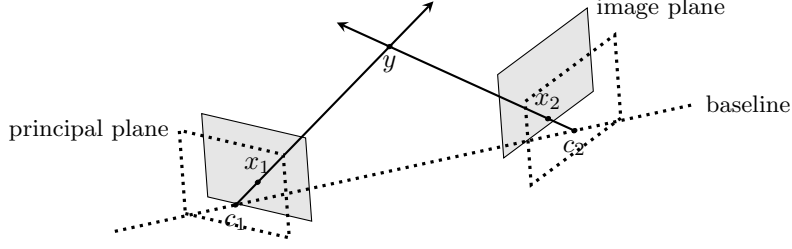


FIGURE 3. Setup of the 2-camera triangulation problem. The world coordinates of the point $y \in \mathbb{R}^3$ are to be reconstructed from the projections $x_1, x_2 \in \mathbb{R}^2$ (in the respective image coordinates) of y onto the image planes of the cameras with centers at c_1 and c_2 (in world coordinates) respectively.

no projection⁴ onto the image plane of the ℓ -th camera, which occurs precisely when y lies on the *principal plane* of the camera [18, p. 160]. This is the plane parallel to the image plane through the camera center c_ℓ ; see Figure 3. It is also known that points on the baseline of two cameras, i.e., the line connecting the camera centers visualised by the dashed line in Figure 3, all project to the same two points on the two cameras, called the epipoles [18, Section 10.1]. Such points cannot be triangulated from only two images. For simplicity, let $\mathcal{B} \subset \mathbb{R}^3$ be the union of the principal planes of the first two cameras and their baseline, so \mathcal{B} is a 2-dimensional subvariety. The next result shows that a subset of the consistent point correspondences outside of \mathcal{B} forms a smooth embedded submanifold of \mathbb{R}^{2r} .

Lemma 6. *Let $\mathcal{O}_{MV} = \mathbb{R}^3 \setminus \mathcal{B}$ with \mathcal{B} as above. The map $\mu_r : \mathcal{O}_{MV} \rightarrow \mathbb{R}^{2r}$ is a diffeomorphism onto its image $\mathcal{I}_{MV} = \mu_r(\mathcal{O}_{MV})$.*

Proof. Clearly μ_r is a smooth map between manifolds ($c_\ell^T y + d_\ell = z_3^\ell \neq 0$). It only remains to show that it has a smooth inverse. Theorem 4.1 of [19] states that μ_2 's projectivization is a birational map, entailing that μ_2 is a diffeomorphism onto its image. Let $\pi_{1:4} : \mathbb{R}^{2r} \rightarrow \mathbb{R}^4$ denote projection onto the first 4 coordinates. Then, $\mu_2^{-1} \circ \pi_{1:4}$ is a smooth map such that $(\mu_2^{-1} \circ \pi_{1:4}) \circ \mu_2 = \mu_2^{-1} \circ \mu_2 = \mathbf{1}_{\mathcal{O}_{MV}}$, having used that the domain \mathcal{O}_{MV} is the same for all r . For the right inverse, we see that any element of \mathcal{I}_{MV} can be written as $\mu_r(y)$ for some $y \in \mathcal{O}_{MV}$. Hence,

$$(\mu_r \circ (\mu_2^{-1} \circ \pi_{1:4}))(\mu_r(y)) = (\mu_r \circ \mathbf{1}_{\mathcal{O}_{MV}})(y) = \mu_r(y),$$

so that it is the identity on \mathcal{I}_{MV} . This proves that μ_r has $\mu_2^{-1} \circ \pi_{1:4}$ as smooth inverse. \square \square

As μ_r^{-1} is required in the statement of the Weingarten map, we give an algorithm for computing $\mu_r^{-1} = \mu_2^{-1} \circ \pi_{1:4}$. Assume that we are given $x \in \mathcal{I}_{MV} \subset \mathbb{R}^{2r}$ in the r -camera multiview manifold and let its first four coordinates be (x_1, y_1, x_2, y_2) . Then, by classic results [18, Section 12.2], the unique element in the kernel of

$$\begin{bmatrix} (x_1 e_3^T - e_1^T) P_1 \\ (y_1 e_3^T - e_2^T) P_1 \\ (x_2 e_3^T - e_1^T) P_2 \\ (y_2 e_3^T - e_1^T) P_2 \end{bmatrix} \in \mathbb{R}^{4 \times 4}$$

yields homogeneous coordinates of the back-projected point in \mathbb{R}^3 .

The solution manifold $\mathcal{S}_{MV} \subset \mathcal{I}_{MV} \times \mathcal{O}_{MV}$ is the graph of μ_r^{-1} . Therefore, it is a properly embedded smooth submanifold; see, e.g., [25, Proposition 5.7].

⁴Actually, it has a projection if we allow points at infinity, i.e., if we consider the triangulation problem in projective space.

8.2. The second fundamental form. Vector fields and integral curves on \mathcal{I}_{MV} can be viewed through the lens of μ_r : We construct a local smooth frame of \mathcal{I}_{MV} by pushing forward a frame from \mathcal{O}_{MV} by μ_r . Then, the integral curves of each of the local smooth vector fields are computed, after which we apply the Gauss formula for curves [24, Lemma 8.5] to compute the second fundamental form.

Because of Lemma 6 a local smooth frame for the *multiview manifold* $\mathcal{I}_{\text{MV}} \subset \mathbb{R}^{2r}$ is obtained by pushing forward the constant global smooth orthonormal frame (e_1, e_2, e_3) of \mathbb{R}^3 by the derivative of μ_r . Its derivative is

$$D_y \mu_r : T_y \mathcal{O}_{\text{MV}} \rightarrow T_{\mu_r(y)} \mathcal{I}_{\text{MV}}, \quad \dot{y} \mapsto \left[\frac{A_\ell \dot{y}}{c_\ell^T y + d_\ell} - (c_\ell^T \dot{y}) \frac{A_\ell y + b_\ell}{(c_\ell^T y + d_\ell)^2} \right]_{\ell=1}^r,$$

and so a local smooth frame of \mathcal{I}_{MV} is given by

$$E_i : \mathcal{I}_{\text{MV}} \rightarrow T\mathcal{I}_{\text{MV}}, \quad \mu_r(y) \mapsto \left[\frac{A_\ell e_i}{c_\ell^T y + d_\ell} - c_{\ell,i} \frac{A_\ell y + b_\ell}{(c_\ell^T y + d_\ell)^2} \right]_{\ell=1}^r, \quad i = 1, 2, 3,$$

where $c_{\ell,i} = c_\ell^T e_i$. It is generally neither orthonormal nor orthogonal.

We compute the second fundamental form of the multiview manifold by differentiation along the integral curves generated by the smooth local frame (E_1, E_2, E_3) . The integral curves through $\mu_r(y)$ generated by this frame are the images of the integral curves passing through y generated by the e_i 's due to [25, Proposition 9.6]. The latter are seen to be $g_i(t) = y + te_i$ by elementary results on linear differential equations. Therefore, the integral curves generated by E_i are

$$\gamma_i(t) = \mu_r(g_i(t)) = \left[\frac{A_\ell(y + te_i) + b_\ell}{c_\ell^T(y + te_i) + d_\ell} \right]_{\ell=1}^r.$$

The components of the second fundamental form at $x = \mu_r(y) \in \mathcal{I}_{\text{MV}}$ are then

$$\begin{aligned} II_x(E_i, E_j) &= P_{N\mathcal{I}_{\text{MV}}} \left(\frac{d}{dt} E_j \Big|_{\gamma_i(t)} \right) \\ &= P_{N\mathcal{I}_{\text{MV}}} \left(\frac{d}{dt} \left[\frac{A_\ell e_j}{c_\ell^T(y + te_i) + d_\ell} - c_{\ell,j} \frac{A_\ell(y + te_i) + b_\ell}{(c_\ell^T(y + te_i) + d_\ell)^2} \right]_{\ell=1}^r \right) \\ &= P_{N\mathcal{I}_{\text{MV}}} \left(\left[-\frac{c_{\ell,i}}{\alpha_\ell^2(y)} A_\ell e_j - \frac{c_{\ell,j}}{\alpha_\ell^2(y)} A_\ell e_i + 2 \frac{c_{\ell,i} c_{\ell,j}}{\alpha_\ell^3(y)} (A_\ell y + b_\ell) \right]_{\ell=1}^r \right), \end{aligned}$$

where $\alpha_\ell(y) = c_\ell^T y + d_\ell$ and $i, j = 1, 2, 3$.

8.3. A practical algorithm. The Weingarten map of \mathcal{I}_{MV} in the direction of the normal vector $\eta \in N_x \mathcal{I}_{\text{MV}}$ is obtained by contracting the second fundamental form with η ; that is, $\widehat{S}_\eta = \langle II_x(E_i, E_j), \eta \rangle$. This can be computed efficiently using linear algebra operations. Partitioning $\eta = [\eta_\ell]_{\ell=1}^n$ with $\eta_\ell \in \mathbb{R}^2$, the symmetric coefficient matrix of the Weingarten map relative to the frame $\mathcal{E} = (E_1, E_2, E_3)$ becomes

$$\widehat{S}_\eta = \left[\sum_{\ell=1}^n 2 \frac{c_{\ell,i} c_{\ell,j}}{\alpha_\ell^3(y)} \eta_\ell^T (A_\ell y + b_\ell) - \frac{c_{\ell,i}}{\alpha_\ell^2(y)} \eta_\ell^T A_\ell e_j - \frac{c_{\ell,j}}{\alpha_\ell^2(y)} \eta_\ell^T A_\ell e_i \right]_{i,j=1}^3,$$

where $y = \mu_r^{-1}(x)$.

In order to compute the spectrum of the Weingarten map using efficient linear algebra algorithms, we need to express it with respect to an orthonormal local smooth frame by applying Gram–Schmidt orthogonalization to \mathcal{E} . This is accomplished by placing the tangent vectors E_1, E_2, E_3 as columns of a $2n \times 3$ matrix J and computing its QR decomposition $QR = J$. The coefficient matrix of the Weingarten map expressed with respect to the orthogonalized frame $Q = (Q_1, Q_2, Q_3)$ is then $S_\eta = R^{-T} \widehat{S}_\eta R^{-1}$. Indeed, R^{-T} maps the basis (E_1, E_2, E_3) to the orthonormal basis (Q_1, Q_2, Q_3) .

Since $\mu_r : \mathcal{O}_{\text{MV}} \rightarrow \mathcal{I}_{\text{MV}}$ is a diffeomorphism, $(D_{(x,y)} \pi_{\mathcal{O}_{\text{MV}}}) (D_{(x,y)} \pi_{\mathcal{I}_{\text{MV}}})^{-1}$ equals the inverse of the derivative of μ_r . As R is the matrix of $D_y \mu_r : T_y \mathcal{O}_{\text{MV}} \rightarrow T_x \mathcal{I}_{\text{MV}}$

expressed with respect to the orthogonal basis (Q_1, Q_2, Q_3) of \mathcal{I}_{MV} and the standard basis of \mathbb{R}^3 , we get that $\kappa_{\text{GCPP}}(x + \eta, x, y)$ equals

$$\begin{aligned} \|(D_{(x,y)}\pi_{\mathcal{O}_{MV}})(D_{(x,y)}\pi_{\mathcal{I}_{MV}})^{-1}(\mathbf{1} - S_\eta)^{-1}\| &= \|R^{-1}(I_3 - S_\eta)^{-1}\|_2 \\ &= \frac{1}{\sigma_3((I - S_\eta)R)}, \end{aligned}$$

where I is the 3×3 identity matrix, and σ_3 is the third largest singular value.

8.4. Numerical experiments. The above computations were implemented in Matlab R2017b [28]. The code we used is provided as supplementary files accompanying the arXiv version of this article. It uses functionality from Matlab’s optimization toolbox. The experiments were performed on a computer running Ubuntu 18.04.3 LTS that consisted of an Intel Core i7-5600U CPU with 8GB main memory.

We present a few numerical examples illustrating the behavior of the condition number of triangulation. The basic setup is described next. We take the 10 camera matrices $P_i \in \mathbb{R}^{3 \times 4}$ from the “model house” data set of the Visual Geometry Group of the University of Oxford [45]. These cameras are all pointing roughly in the same direction. In our experiments we reconstruct the point $y := p + 1.5^{10}v \in \mathbb{R}^3$, where $p = (-1.85213, -0.532959, -5.65752) \in \mathbb{R}^3$ is one point of the house and $v = (-0.29292, -0.08800, -0.95208)$ is the unit-norm vector that points from the center of the first camera p . Given a data point $a \in \mathbb{R}^{2r}$, it is triangulated as follows. First a linear triangulation method is applied, finding the right singular vector corresponding to the least singular value of a matrix whose construction is described (for two points) in [18, Section 12.2]. We then use it as a starting point for solving optimization problem (11) with Matlab’s nonlinear least squares solver `lsqnonlin`. For this solver, the following settings were used: `TolFun` and `TolX` set to 10^{-28} , `StepTolerance` equal to 10^{-14} , and both `MaxFunEvals` and `MaxIter` set to 10^4 . We provided the Jacobian to the algorithm, which it can evaluate numerically.

8.4.1. Experiment 1. In the first experiment, we provide numerical evidence for the correctness of our theoretical results. We project y to the image planes of the $r = 10$ cameras: $x = \mu_r(y)$. A random normal direction $\eta \in N_x \mathcal{I}_{MV}$ is sampled by taking a random vector with i.i.d. standard normal entries, projecting it to the normal space, and then scaling it to unit norm. We investigate the sensitivity of the points along the ray $a(t) := x - t\eta$.

The theoretical condition number of the triangulation problem at $a(t)$ can be computed numerically for every t using the algorithm from Section 8.3. We can also estimate the condition number experimentally, for example by generating a large number of small perturbations $a(t) + E(t)$ with $\|E(t)\| \approx 0$, approximately solving (11) numerically using `lsqnonlin` and then checking the distance to the true critical point y . However, from the theory we know that the worst direction of infinitesimal perturbation is given by the left singular vector of $(I - S_{-t\eta})R$ corresponding to the smallest (i.e. third) singular value, where R is as in Section 8.3. Let $u(t) \in \mathbb{R}^3$ denote this vector, which contains the coordinates of the perturbation relative to the orthonormal basis $Q = (Q_1, Q_2, Q_3)$; see Section 8.3. Then, it suffices to consider only a small (relative) perturbation in this direction; we took $E(t) := 10^{-6}\|a(t)\|Qu(t)$. We solve (11) with input $a(t) + E(t)$ and output $y_{\text{est}}(t)$ using `lsqnonlin` with the exact solution of the unperturbed problem y as starting point. The experimental estimate of the condition number is then $\kappa_{\text{est}}(t) = \frac{\|y - y_{\text{est}}(t)\|}{\|E(t)\|}$.

In Figure 4 we show the experimental results for the above setup, where we chose $t = 10^i\|x\|$ with 100 values of i uniformly spaced between -3 and 2 . It is visually evident that the experimental results support the theory. Excluding the three last

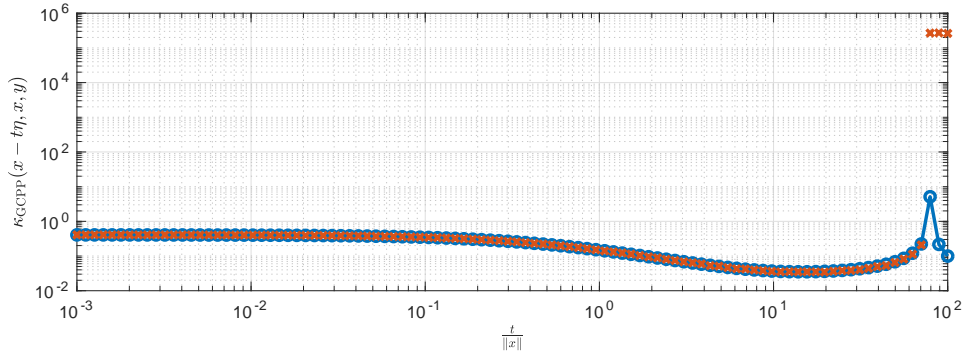


FIGURE 4. A comparison of theoretical and experimental data of the condition number of the triangulation problem with all cameras for several points along the ray $x - t\eta$. Herein, η is a randomly chosen unit-norm normal direction at $x \in \mathcal{I}_{\text{MV}}$. The numerically computed theoretical condition numbers are indicated by circles, while the experimentally estimated condition numbers, as described in the text, are plotted with crosses.

values of t , the arithmetic and geometric means of the condition number divided by the experimental estimate are approximately 1.006664 and 1.006497 respectively. This indicates a near perfect match with the theory.

There appears to be one anomaly in Figure 4, however: the three red crosses to the right of the singularity at $t^* = 79.64416\|x\|$. What happens is that past the singularity y is no longer a local minimizer of $\min_{y \in \mathcal{O}_{\text{MV}}} \frac{1}{2}\|a(t) - \mu_{10}(y)\|^2$. This is because $x(t)$ is no longer a local minimizer of $\min_{x \in \mathcal{I}_{\text{MV}}} \frac{1}{2}\|a(t) - x\|^2$. Since we are applying an optimization method, the local minimizer happens to move away from the nearby critical point and instead converges to a different point. Indeed, one can show that the Riemannian Hessians (see [2, Chapter 5.5]) of these problems are positive definite for small t , but become indefinite past the singularity t^* .

8.4.2. Experiment 2. The next experiment illustrates how the condition number varies with the distance t along a normal direction $t\eta \in \mathcal{N}\mathcal{I}_{\text{MV}}$. We consider the setup from the previous paragraph. The projection of the point y onto the image planes of the first k cameras is $x_k := \mu_k(y) = (P_1 y, \dots, P_k y)$. A random unit-norm normal vector η_k in $\mathcal{N}_{x_k} \mathcal{I}_{\text{MV}}$ is chosen as described before. We investigate the sensitivity of the perturbed inputs $a_k(t) := x_k + t\eta_k$ for $t \in \mathbb{R}$. The condition number is computed for these inputs for $k = 2, 3, 5, 10$ and $\frac{\pm t}{\|x_k\|} = 10^i$ for 10^4 values of i uniformly spaced between -3 and 4 . The results are shown in Figure 5. We have 3 peaks for a fixed k because $\dim \mathcal{I}_{\text{MV}} = 3$. The two-camera system only has two singularities in the range $|t| < 10^4 \|x_2\|$. Note that these figures illustrate the continuity of κ_{GCPP} as in Corollary 4.

Up to about $|t| \leq 10^{-2} \|x_k\|$ we observe that curvature hardly affects the condition number of the GCPP for the triangulation problem. Beyond this value, curvature plays the dominant role: both the singularities and the tapering off for high relative errors are caused by it. Moreover, the condition number decreases as the number of cameras increases. This indicates that the use of *minimal problems* [23] in computer vision could potentially introduce numerical instability.

8.4.3. Experiment 3. We investigate the influence of the number of cameras on the condition number of the triangulation problem. We consider points lying on a circle in \mathbb{R}^3 around the point p of the house. Specifically, we take the unit circle $C = \{p + (\cos(\theta), \sin(\theta), 1) \mid \theta \in [0, 2\pi]\}$. We take 100 points $y_{\theta_j} \in C$ uniformly

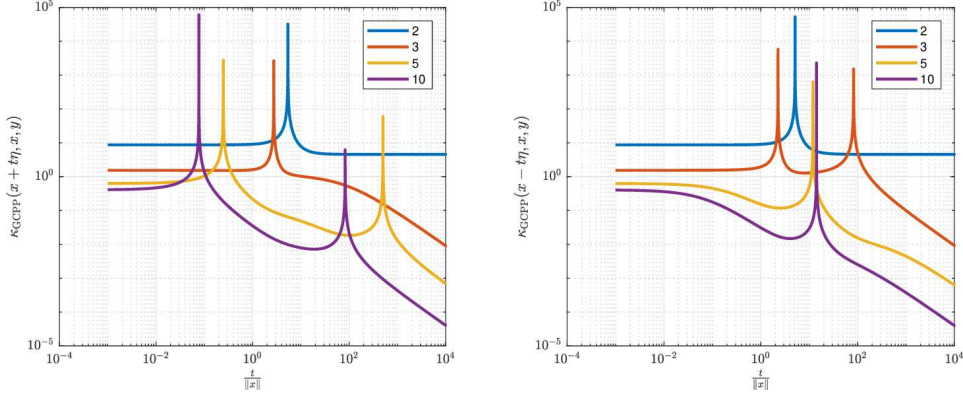


FIGURE 5. The GCPP condition number in function of the relative distance $\frac{t}{\|x\|}$ from a specified $x \in \mathcal{I}_{MV}$ and a randomly chosen unit-length normal direction η . Each of the four lines corresponds to a different number k of cameras taking the pictures, namely $k = 2, 3, 5, 10$.

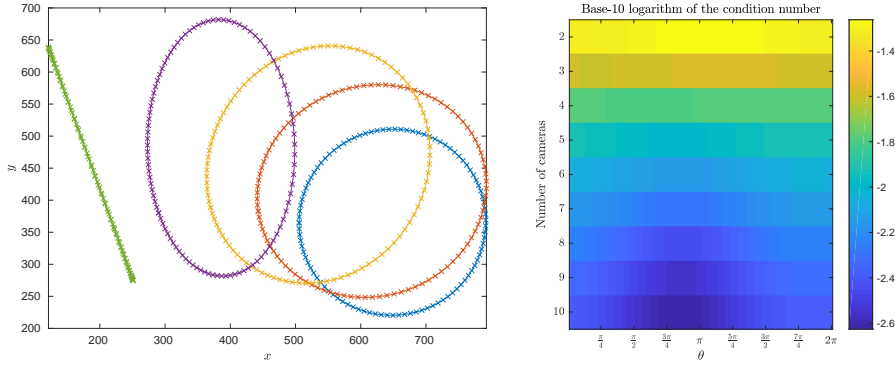


FIGURE 6. The left subplot shows overlaid pictures taken by the cameras P_1, P_3, P_5, P_7 , and P_9 of a unit circle C around a specific point in \mathbb{R}^3 . The right subplot displays the base-10 logarithm of the condition number of the triangulation problem with the first k cameras, for $k = 2, \dots, 10$, for several points on the circle C .

spaced on this circle. The left plot in Figure 6 shows the pictures of the points y_{θ_j} taken by five different cameras in the data set in one plot.

For $k = 2, \dots, 10$, we apply the first k projection matrices P_i to y_{θ_j} , obtaining $x_{k,j} = (P_1 y_{\theta_j}, \dots, P_k y_{\theta_j}) \in \mathcal{I}_{MV}$. We sample random directions $\eta_{k,j} \in \mathbb{N}_{x_{k,j}} \mathcal{I}_{MV}$ as before. To determine the condition number, we triangulate the point $a_{k,j} := x_{k,j} + 10^{-2} \eta_{k,j}$, yielding $y'_{k,j} \in \mathbb{R}^3$. The point $y'_{k,j}$ is projected again to the cameras to obtain $x'_{k,j} \approx x_{k,j}$. The condition number $\kappa_{GCPP}(a_{k,j}, x'_{k,j}, y'_{k,j})$ is then computed using the algorithm from the previous subsection for all k and j . The results are displayed on the right in Figure 6. The decrease in condition as the number of cameras increases is evident. We also observe that with many cameras the condition number seems to decrease further for θ_j between $\frac{3}{4}\pi$ and π . The reason seems to be that the points y_{θ_j} are closer to most of the cameras in this case than at $\theta = 0$.

8.4.4. *Experiment 4.* In the final experiment we investigate the relation between the distance of a point in the output space \mathbb{R}^3 and the centers of the cameras. Intuitively

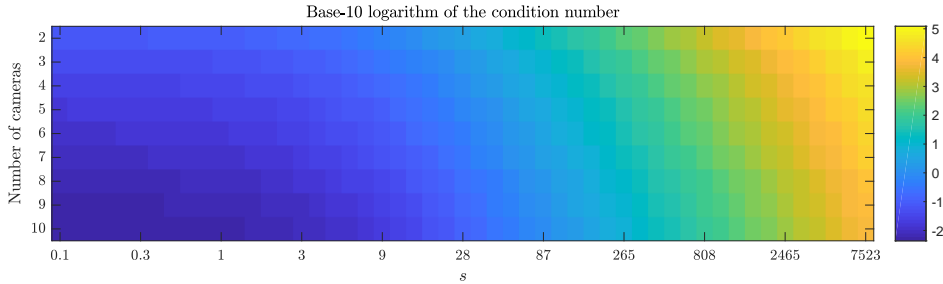


FIGURE 7. The base-10 logarithm of the condition number of the triangulation problem with the first k cameras, for $k = 2, \dots, 10$, for several points on the ray $y(s) = y + sv \in \mathbb{R}^3$. The choice of $y \in \mathbb{R}^3$ and the direction v is discussed in the text.

one can expect that triangulating a point y farther from the cameras should be more sensitive to absolute perturbations of the coordinates of the projections $P_i y$, because a small perturbation on the image plane (i.e., a small angular error) is backprojected along a long ray. In order to test this hypothesis, we consider points $y(s) := y + sv \in \mathbb{R}^3$ for $s \in [0, \infty)$, where y and v are as before. We use the camera projection matrices P_i to determine the corresponding point $x(s) \in \mathcal{I}_{MV}$, then choose a random normal direction $\eta(s)$ as before and set $a(s) = x(s) + 10^{-2}\eta(s)$. The condition number is determined using the algorithm from Section 8.3. We perform these computations for the distances $s_i = 1.25^i$ for $i = -10, -9, \dots, 40$ and also for a varying number of cameras $k = 2, \dots, 10$ as before. The results of this experiment are shown in Figure 7. They clearly support the hypothesis that as the world point lies farther from all cameras, the sensitivity of the triangulation problem increases.

ACKNOWLEDGEMENTS

The authors wish to thank Nicolas Boumal for posing a question on unconstrained errors, which eventually started the project that led to this article. We are greatly indebted to Carlos Beltrán who meticulously studied the manuscript and asked pertinent questions about the theory. Furthermore, the authors would like to thank Peter Bürgisser for hosting the second author at TU Berlin in August 2019, and Joeri Van der Veken for fruitful suggestions and pointers to the literature.

APPENDIX A. PROOFS OF THE MAIN RESULTS

This section contains our proofs of the theorems. The order is as follows. First we prove the results from Section 4. Then, we prove the results from Section 5. Finally, we prove the results from Section 3.

A.1. Proofs for Section 4.

Proof of Lemma 2. Recall that $\mathcal{S}_{\text{CPP}} = \{(a, x) \in \mathbb{R}^n \times \mathcal{I} \mid x - a \in N_x \mathcal{I}\}$, and that the normal bundle of \mathcal{I} is denoted by $N\mathcal{I}$. Consider the map $\psi : N\mathcal{I} \rightarrow \mathbb{R}^n \times \mathbb{R}^n$ sending (x, η) to $(x + \eta, x)$. Since ψ is the restriction of the invertible linear map $\Phi : \mathbb{R}^n \times \mathbb{R}^n \rightarrow \mathbb{R}^n \times \mathbb{R}^n$, $(x, y) \mapsto (x + y, x)$, we see that ψ has maximal rank n , so it is a smooth immersion, and that ψ is injective. Since $N\mathcal{I}$ is a smooth manifold in the subspace topology of $\mathbb{R}^n \times \mathbb{R}^n$, ψ is also an open map relative to the subspace topologies on its domain and codomain. It follows from [25, Proposition 4.22(a)] that ψ is a smooth embedding. Hence, the image $\psi(N\mathcal{I}) = \mathcal{S}_{\text{CPP}}$ is an embedded submanifold by [25, Proposition 5.2]. \square \square

Proof of Lemma 3. Recall that $\Pi_{\mathbb{R}^n}$ is a smooth map, so if its derivative is nonsingular at a point $(a, x) \in \mathcal{S}_{\text{CPP}}$, then there exists an open neighborhood of (a, x) where this property remains valid. Therefore, applying the inverse function theorem [25, Theorem 4.5] at $(a, x) \in \mathcal{W}_{\text{CPP}}$, the fact that $D_{(a,x)}\Pi_{\mathbb{R}^n}$ is invertible implies that there is a neighborhood $\mathcal{N}_{(a,x)}$ of (a, x) in \mathcal{W}_{CPP} and a neighborhood of a in \mathbb{R}^n such that $\mathcal{N}_{(a,x)}$ is diffeomorphic to (an open ball in) \mathbb{R}^n . Hence, \mathcal{W}_{CPP} is open in \mathcal{S}_{CPP} , and, hence, it is an open submanifold of dimension n .

To show that \mathcal{W}_{CPP} is dense in \mathcal{S}_{CPP} , take any $(a, x) \in \mathcal{S}_{\text{CPP}} \setminus \mathcal{W}_{\text{CPP}}$. Let $\eta = a - x$. Then, $(x, x) + (\alpha\eta, 0) \in \mathcal{S}_{\text{CPP}}$ because $\eta \in N_x\mathcal{I}$. By Lemma 5, $(x, x) + (\alpha\eta, 0) \in \mathcal{W}_{\text{CPP}}$ with $\alpha \in (0, \infty)$ if and only if $\mathbf{1} - S_{\alpha\eta} = \mathbf{1} - \alpha S_\eta$ is singular. The latter is singular iff $S_\eta - \frac{1}{\alpha}\mathbf{1}$ is singular. This occurs only if $\frac{1}{\alpha}$ equals one of the at most $m = \dim \mathcal{I}$ eigenvalues of the Weingarten map S_η . Consequently, (a, x) can be reached as the limit of a sequence $(x, x) + (\alpha_n\eta, 0)$, which is wholly contained in \mathcal{W}_{CPP} by taking α_n outside of the discrete set.

Applying [25, Proposition 5.1], we can conclude that \mathcal{W}_{CPP} is even an embedded submanifold. This concludes the argument. \square \square

Proof of Theorem 2. Let $(a, x) \in \mathcal{W}_{\text{CPP}}$ be arbitrary. On \mathcal{W}_{CPP} , the coordinate projection $\Pi_{\mathbb{R}^n} : \mathcal{S}_{\text{CPP}} \rightarrow \mathbb{R}^n$ has an invertible derivative. Consequently, by the inverse function theorem [25, Theorem 4.5] there exist open neighborhoods $\mathcal{X} \subset \mathcal{S}_{\text{CPP}}$ of (a, x) and \mathcal{Y} of $a \subset \mathbb{R}^n$ such that $\Pi_{\mathbb{R}^n}|_{\mathcal{X}} : \mathcal{X} \rightarrow \mathcal{Y}$ has a smooth inverse function that we call $\phi_{(a,x)}$. Its derivative is $D_a\phi_{(a,x)} = (D_{(a,x)}\Pi_{\mathbb{R}^n})^{-1}$. Consider the smooth map $\Phi_{(a,x)} := \Pi_{\mathcal{I}} \circ \phi_{(a,x)}$, where $\Pi_{\mathcal{I}} : \mathcal{S}_{\text{CPP}} \rightarrow \mathcal{I}$ is the coordinate projection. The CPP condition number at $(a, x) \in \mathcal{W}_{\text{CPP}}$ was defined exactly as $\kappa[\Phi_{(a,x)}](a)$. By [34, Theorem 4] we have that $\kappa[\Phi_{(a,x)}](a) = \kappa_{\text{CPP}}(a, x) = \|D_a\Phi_{(a,x)}\|$. Since $D_a\Phi_{(a,x)} = (D_{(a,x)}\Pi_{\mathcal{I}})(D_{(a,x)}\Pi_{\mathbb{R}^n})^{-1}$, we have that $\kappa_{\text{CPP}}(a, x) = \|(D_{(a,x)}\Pi_{\mathcal{I}})(D_{(a,x)}\Pi_{\mathbb{R}^n})^{-1}\|$. It follows from Lemma 5 and (10) that we have $(D_{(a,x)}\Pi_{\mathcal{I}})(D_{(a,x)}\Pi_{\mathbb{R}^n})^{-1} = (\mathbf{1} - S_\eta)^{-1}P_{T_x\mathcal{I}}$. This concludes the first part. The second part is Lemma 5. \square \square

A.2. Proofs for Section 5.

Proof of Lemma 4. Combining Assumption 1 and Lemma 3, we see that $\mathcal{W}_{\text{GCCPP}}$ is realized as the intersection of two smoothly embedded product manifolds:

$$\mathcal{W}_{\text{GCCPP}} = (\mathcal{W}_{\text{CPP}} \times \mathcal{O}) \cap (\mathbb{R}^n \times \mathcal{W}) \subset \mathbb{R}^n \times \mathcal{I} \times \mathcal{O}.$$

Note that $\text{codim}(\mathcal{W}_{\text{CPP}} \times \mathcal{O}) = \dim \mathcal{I}$, by Lemma 2, and $\text{codim}(\mathbb{R}^n \times \mathcal{W}) = \dim \mathcal{O}$, because $\dim \mathcal{W} = \dim \mathcal{S}$ and Assumption 1 stating that $\dim \mathcal{S} = \dim \mathcal{I}$. Thus, it suffices to prove that the intersection is *transversal* [25, Theorem 6.30], because then $\mathcal{W}_{\text{GCCPP}}$ would be an embedded submanifold of codimension $\dim \mathcal{I} + \dim \mathcal{O}$.

Consider a point $(a, x, y) \in \mathcal{W}_{\text{GCCPP}}$. Transversality means that we need to show

$$T_{(a,x,y)}(\mathcal{W}_{\text{CPP}} \times \mathcal{O}) + T_{(a,x,y)}(\mathbb{R}^n \times \mathcal{W}) = T_{(a,x,y)}(\mathbb{R}^n \times \mathcal{I} \times \mathcal{O}).$$

Fix an arbitrary $(\dot{a}, \dot{x}, \dot{y}) \in T_a\mathbb{R}^n \times T_x\mathcal{I} \times T_y\mathcal{O}$. Then, it suffices to show there exist $((\dot{a}_1, \dot{x}_1), \dot{y}_1) \in T_{(a,x)}\mathcal{W}_{\text{CPP}} \times T_y\mathcal{O}$ and $(\dot{a}_2, (\dot{x}_2, \dot{y}_2)) \in T_a\mathbb{R}^n \times T_{(x,y)}\mathcal{W}$ such that $(\dot{a}, \dot{x}, \dot{y}) = (\dot{a}_1 + \dot{a}_2, \dot{x}_1 + \dot{x}_2, \dot{y}_1 + \dot{y}_2)$. It follows from Corollary 7 and Lemma 5 that $\dot{a}_1 = (\mathbf{1} - S_\eta)\dot{x}_1 + \dot{\eta}$, where $\eta = a - x$ and where $\dot{\eta} \in N_x\mathcal{I}$. The tangent vectors $\dot{y}_1 \in T_y\mathcal{O}$, $\dot{a}_2 \in T_a\mathbb{R}^n$ and $\dot{x}_1 \in T_x\mathcal{I}$ can be chosen freely. Choosing $\dot{x}_1 = \dot{x}$ and $\dot{x}_2 = 0$; $\dot{y}_1 = \dot{y}$ and $\dot{y}_2 = 0$ and $\dot{a}_1 = (\mathbf{1} - S_\eta)\dot{x}_1$ and $\dot{a}_2 = \dot{a} - \dot{a}_1$ yields $(\dot{a}, \dot{x}, \dot{y})$. This concludes the first part of the proof.

It remains to prove $\mathcal{W}_{\text{GCCPP}}$ is dense in $\mathcal{S}_{\text{GCCPP}}$. For this, we recall that

$$\mathcal{S}_{\text{GCCPP}} = (\mathcal{S}_{\text{CPP}} \times \mathcal{O}) \cap (\mathbb{R}^n \times \mathcal{S}).$$

Let $(a, x, y) \in \mathcal{S}_{\text{GCCPP}}$ and let $\eta = a - x \in N_x\mathcal{I}$. Then, $(a, x) \in \mathcal{S}_{\text{CPP}}$ and $(x, y) \in \mathcal{S}$. As \mathcal{W} is an open dense submanifold of \mathcal{S} by Assumption 1, there exists a sequence

$(x_i, y_i) \in \mathcal{W}$ such that $\lim_{i \rightarrow \infty} (x_i, y_i) = (x, y)$. Moreover, there exists a sequence $\eta_i \rightarrow \eta$ with $\eta_i \in \mathbb{T}_{x_i} \mathcal{I}$ so that $(x_i + \eta_i, x_i) \in \mathcal{S}_{\text{CPP}}$, because $\Pi_{\mathcal{I}}(\mathcal{S}_{\text{CPP}}) = \mathcal{I}$. Since \mathcal{W}_{CPP} is open dense in \mathcal{S}_{CPP} by Lemma 3, only finitely many elements of the sequence are not in \mathcal{W}_{CPP} . We can pass to a subsequence $(x_j + \eta_j, x_j) \in \mathcal{W}_{\text{CPP}}$. Now $(x_j + \eta_j, x_j, y_j) \in \mathcal{W}_{\text{GCPP}}$ and moreover its limit is $(x + \eta, x, y) \in \mathcal{S}_{\text{GCPP}}$. This concludes the proof. \square \square

Proof of Theorem 3. By [34, Theorem 4], for a well-posed triple $(a, x, y) \in \mathcal{W}_{\text{GCPP}}$ we have $\kappa_{\text{GCPP}}(a, x, y) = \|(\mathbf{D}_{(a,x,y)} \Pi_{\mathcal{O}})(\mathbf{D}_{(a,x,y)} \Pi_{\mathbb{R}^n})^{-1}\|$. We compute the right hand side of this equation. The situation appears as follows:

$$\begin{array}{ccc} \mathcal{W}_{\text{CPP}} & \xrightarrow{\Pi_{\mathbb{R}^n}} & \mathbb{R}^n & \xleftarrow{\Pi_{\mathbb{R}^n}} & \mathcal{W}_{\text{GCPP}} \\ \Pi_{\mathcal{I}} \downarrow & & & & \downarrow \Pi_{\mathcal{O}} \\ \mathcal{I} & \xleftarrow{\pi_{\mathcal{I}}} & \mathcal{W} & \xrightarrow{\pi_{\mathcal{O}}} & \mathcal{O} \end{array}$$

We have in addition the projections $(\mathbf{1} \times \Pi_{\mathcal{I}}) : \mathcal{W}_{\text{GCPP}} \rightarrow \mathcal{W}_{\text{CPP}}$, $(a, x, y) \mapsto (a, x)$ and $(\Pi_{\mathcal{I}} \times \mathbf{1}) : \mathcal{W}_{\text{GCPP}} \rightarrow \mathcal{W}$, $(a, x, y) \mapsto (x, y)$. With this we have

$$(\Pi_{\mathbb{R}^n} \circ (\mathbf{1} \times \pi_{\mathcal{I}}))(a, x, y) = \Pi_{\mathbb{R}^n}(a, x, y) \quad \text{and} \quad (\pi_{\mathcal{O}} \circ (\Pi_{\mathcal{I}} \times \mathbf{1}))(a, x, y) = \Pi_{\mathcal{O}}(a, x, y).$$

Taking derivatives we get

$$\begin{aligned} \mathbf{D}_{(a,x)} \Pi_{\mathbb{R}^n} \mathbf{D}_{(a,x,y)} (\mathbf{1} \times \pi_{\mathcal{I}}) &= \mathbf{D}_{(a,x,y)} \Pi_{\mathbb{R}^n} \quad \text{and} \\ \mathbf{D}_{(a,x)} \pi_{\mathcal{O}} \mathbf{D}_{(a,x,y)} (\Pi_{\mathcal{I}} \times \mathbf{1}) &= \mathbf{D}_{(a,x,y)} \Pi_{\mathcal{O}}. \end{aligned}$$

Since $(x, y) \in \mathcal{W}$, the derivative $\mathbf{D}_{(x,y)} \pi_{\mathcal{I}}$ is invertible, and so $\mathbf{D}_{(a,x,y)} (\mathbf{1} \times \pi_{\mathcal{I}})$ is also invertible. On other hand, since $(a, x) \in \mathcal{W}_{\text{CPP}}$, the derivative $\mathbf{D}_{(a,x)} \Pi_{\mathbb{R}^n}$ is invertible. Altogether we see that $\mathbf{D}_{(a,x,y)} \Pi_{\mathbb{R}^n}$ is invertible, and that

$$\begin{aligned} &(\mathbf{D}_{(a,x,y)} \Pi_{\mathcal{O}})(\mathbf{D}_{(a,x,y)} \Pi_{\mathbb{R}^n})^{-1} \\ &= (\mathbf{D}_{(x,y)} \pi_{\mathcal{O}}) (\mathbf{D}_{(a,x,y)} (\Pi_{\mathcal{I}} \times \mathbf{1})) (\mathbf{D}_{(a,x,y)} (\mathbf{1} \times \pi_{\mathcal{I}}))^{-1} (\mathbf{D}_{(a,x)} \Pi_{\mathbb{R}^n})^{-1}. \end{aligned}$$

The derivatives in the middle satisfy

$$(\dot{x}, \dot{y}) = \mathbf{D}_{(a,x,y)} (\Pi_{\mathcal{I}} \times \mathbf{1}) (\mathbf{D}_{(a,x,y)} (\mathbf{1} \times \pi_{\mathcal{I}}))^{-1} (\dot{a}, \dot{x}),$$

while on the other hand we have

$$(\dot{x}, \dot{y}) = (\mathbf{D}_{(x,y)} \pi_{\mathcal{I}})^{-1} \mathbf{D}_{(a,x)} \Pi_{\mathcal{I}} (\dot{a}, \dot{x}).$$

This implies that the two linear maps on the right hand side in the previous equations are equal. Hence,

$$\begin{aligned} (12) \quad &(\mathbf{D}_{(a,x,y)} \Pi_{\mathcal{O}})(\mathbf{D}_{(a,x,y)} \Pi_{\mathbb{R}^n})^{-1} = (\mathbf{D}_{(x,y)} \pi_{\mathcal{O}})(\mathbf{D}_{(x,y)} \pi_{\mathcal{I}})^{-1} (\mathbf{D}_{(a,x)} \Pi_{\mathcal{I}})(\mathbf{D}_{(a,x)} \Pi_{\mathbb{R}^n})^{-1} \\ &= (\mathbf{D}_{(x,y)} \pi_{\mathcal{O}})(\mathbf{D}_{(x,y)} \pi_{\mathcal{I}})^{-1} (\mathbf{1} - S_{\eta})^{-1} \mathbf{P}_{\mathbb{T}_x \mathcal{I}}, \end{aligned}$$

where we used (10) and Lemma 5. Taking spectral norms on both sides completes the proof for points in $\mathcal{W}_{\text{GCPP}}$. Finally, for points outside $\mathcal{W}_{\text{GCPP}}$ the proof follows from the definition of $\mathcal{W}_{\text{GCPP}}$ combined with Theorem 1 and 2. \square \square

A.3. Proofs for Section 6.

Proof of Proposition 1. Restricted to the tubular neighborhood \mathcal{T} where (AP) is defined, the unique closest point to the manifold is also the closest critical point. The result follows by substituting $x^* = \mathbf{P}_{\mathcal{I}}(a^*)$ and $x = \mathbf{P}_{\mathcal{I}}(a)$ in Theorem 4, and simplifying the resulting statements by eliminating x and x^* . \square \square

Proof of Proposition 2. Taking the derivative of the objective function at a point $(x, y) \in \mathcal{W}$ we see that the critical points satisfy $\langle a - x, D_{(x,y)}\pi_{\mathcal{I}}(\dot{x}, \dot{y}) \rangle = 0$ for all $(\dot{x}, \dot{y}) \in T_{(x,y)}\mathcal{W}$. By the definition of \mathcal{W} , the derivative $D_{(x,y)}\pi_{\mathcal{I}}$ is surjective, which implies that $(D_{(x,y)}\pi_{\mathcal{I}})(T_{(x,y)}\mathcal{W}) = T_x\mathcal{I}$. Therefore, the condition of being a critical point is equivalent to $a - x \in N_x\mathcal{I}$. \square \square

Proof of Theorem 4. By assumption $(a^*, x^*, y^*) \in \mathcal{W}_{\text{GCPP}}$. In particular, this implies $(a^*, x^*) \in \mathcal{W}_{\text{GCPP}}$, so that $D_{(a^*, x^*)}\Pi_{\mathbb{R}^n} : T_{(a^*, x^*)}\mathcal{W}_{\text{GCPP}} \rightarrow \mathbb{R}^n$ is invertible. By the inverse function theorem [25, Theorem 4.5], there is an open neighborhood $\mathcal{U}_{(a^*, x^*)} \subset \mathcal{W}_{\text{GCPP}}$ of (a^*, x^*) such that $\Pi_{\mathbb{R}^n}$ restricts to a diffeomorphism on

$$\mathcal{A}_{a^*} = \Pi_{\mathbb{R}^n}(\mathcal{U}_{(a^*, x^*)}).$$

Let $\Pi_{\mathbb{R}^n}^{-1}$ denote the inverse of $\Pi_{\mathbb{R}^n}$ on \mathcal{A}_{a^*} . Combining (10) and Lemma 5, the derivative of $\Pi_{\mathcal{I}} \circ \Pi_{\mathbb{R}^n}^{-1}$ is given by

$$(D_{(a,x)}\Pi_{\mathcal{I}})(D_{(a,x)}\Pi_{\mathbb{R}^n})^{-1} = (\mathbf{1} - S_\eta)^{-1}P_{T_x\mathcal{I}}$$

and thus has constant rank on \mathcal{A}_{a^*} equal to $\dim \mathcal{I}$. This implies that

$$(\mathbf{1} \times D_{(x,y)}\pi_{\mathcal{O}} D_{(x,y)}\pi_{\mathcal{I}}^{-1})(D_{(a,x)}\Pi_{\mathcal{I}})(D_{(a,x)}\Pi_{\mathbb{R}^n})^{-1} : T_a\mathcal{A}_{a^*} \rightarrow T_{(x,y)}\mathcal{W}$$

has constant rank on \mathcal{A}_{a^*} equal to $\dim \mathcal{I} = \dim \mathcal{W}$, by Assumption 1. Consequently, there is a smooth function

$$\Phi : \mathcal{A}_{a^*} \rightarrow \mathcal{W}$$

with $\Phi(a^*) = (x^*, y^*)$. In fact, the above has already shown that its derivative has constant rank equal to $\dim \mathcal{W}$. Therefore, Φ is a smooth submersion. Now, by Proposition 4.28 of [25], $\Phi(\mathcal{A}_{a^*}) \subset \mathcal{W}$ is an open subset, so it is a submanifold of dimension $\dim \mathcal{I} = \dim \mathcal{W}$. Similarly, the derivative $D_{(x,y)}\pi_{\mathcal{I}}$ at $(x, y) \in \mathcal{W}$ has maximal rank equal to $\dim \mathcal{I}$, by definition of \mathcal{W} . Hence, $\pi_{\mathcal{I}} \circ \Phi$ is also a smooth submersion. Therefore, after possibly passing to an open subset of \mathcal{A}_{a^*} , we can assume that

$$\mathcal{N}_{(x^*, y^*)} := \Phi(\mathcal{A}_{a^*}) \subset \mathcal{W} \quad \text{and} \quad \mathcal{I}_{x^*} = \pi_{\mathcal{I}}(\mathcal{N}_{(x^*, y^*)}) \subset \mathcal{I}$$

are open submanifolds each of dimension $\dim \mathcal{I}$ and that

- (i) x^* is the global minimizer of the distance to a^* on \mathcal{I}_{x^*} , and hence,
- (ii) all $x \in \mathcal{I}_{x^*}$ lie on the same side of $T_{x^*}\mathcal{I}_{x^*}$, considering the tangent space $T_{x^*}\mathcal{I}_{x^*}$ as an affine linear subspace of \mathbb{R}^n with base point x^* .

Now let $a \in \mathcal{A}_{a^*}$ be a point in the neighborhood of a^* . The restricted squared distance function $d_a : \mathcal{N}_{(x^*, y^*)} \rightarrow \mathbb{R}$, $(x, y) \mapsto \frac{1}{2}\|a - \pi_{\mathcal{I}}(x, y)\|^2$ that is minimized on $\mathcal{N}_{(x^*, y^*)}$ is smooth. Its critical points satisfy

$$\langle a - \pi_{\mathcal{I}}(x, y), D_{(x,y)}\pi_{\mathcal{I}}(\dot{x}, \dot{y}) \rangle = 0 \quad \text{for all} \quad (\dot{x}, \dot{y}) \in T_{(x,y)}\mathcal{N}_{(x^*, y^*)}.$$

Since $(x^*, y^*) \in \mathcal{N}_{(x^*, y^*)} \subset \mathcal{W}$, the derivative $D_{(x^*, y^*)}\pi_{\mathcal{I}}$ of $\pi_{\mathcal{I}} : \mathcal{W} \rightarrow \mathcal{I}$ is invertible. Then, for all $(x, y) \in \mathcal{N}_{(x^*, y^*)}$ the image of $D_{(x,y)}\pi_{\mathcal{I}}$ is the whole tangent space $T_x\mathcal{I}$. Consequently, the critical points must satisfy $a - x \perp T_x\mathcal{I}$.

By construction, for every $a \in \mathcal{A}_{a^*}$ there is a unique $(x, y) \in \mathcal{N}_{(x^*, y^*)}$ so that $(a, x, y) \in \mathcal{W}_{\text{GCPP}}$, namely $(x, y) = \Phi(a)$. This implies that (x, y) is the *unique* critical point of the squared distance function restricted to $\mathcal{N}_{(x^*, y^*)}$.

It only remains to show that for all $a \in \mathcal{A}_{a^*}$, the minimizer of d_a is attained in the interior of $\mathcal{N}_{(x^*, y^*)}$. This would entail that the unique critical point is also the unique global minimizer on $\mathcal{N}_{(x^*, y^*)}$. We show that there exists a $\delta > 0$ such that restricting \mathcal{A}_{a^*} to the open ball $B_\delta(a^*)$ of radius δ centered at a^* in \mathbb{R}^n yields the desired result.

Here is the geometric setup for the rest of the proof, depicted in Figure 8: let $a \in B_\delta(a^*)$ and let $(x, y) \in \overline{\mathcal{N}_{(x^*, y^*)}}$ be the minimizer for d_a in the closure of $\mathcal{N}_{(x^*, y^*)}$. Then, x is in the closure of \mathcal{I}_{x^*} by continuity of $\pi_{\mathcal{I}}$. Furthermore, let

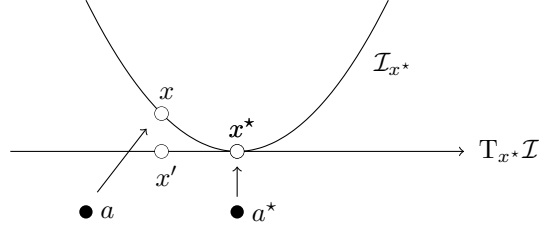


FIGURE 8. A sketch of the geometric construction in the proof of Theorem 4.

$x' = P(x)$, where $P := P_{\mathbb{T}_{x^*}\mathcal{I}_{x^*}}$ is the orthogonal projection onto the tangent space $\mathbb{T}_{x^*}\mathcal{I}^*$ considered as an affine linear subspace of \mathbb{R}^n with base point x^* .

The image of $B_\delta(a^*)$ under P is an open ball $B_\delta(x^*) \cap \mathbb{T}_{x^*}\mathcal{I}_{x^*} \subset \mathbb{T}_{x^*}\mathcal{I}_{x^*}$. The distance function $h : \mathcal{I}_{x^*} \rightarrow \mathbb{R}$, $x \mapsto \|x - P(x)\|$ measures the “height” of x from the tangent space $\mathbb{T}_{x^*}\mathcal{I}_{x^*}$. Now, we can bound the distance from a to x as follows.

$$\begin{aligned}
 \|a - x\| &= \|a - a^* + a^* - x^* + x^* - x' + x' - x\| \\
 &\leq \|a - a^*\| + \|a^* - x^*\| + \|x^* - x'\| + \|x - x'\| \\
 &\leq \|a^* - x^*\| + 2\delta + h(x) \\
 (13) \quad &\leq \|a^* - x^*\| + 2\delta + \max_{z \in \mathcal{P}_\delta(x^*)} h(z),
 \end{aligned}$$

where the first bound is the triangle inequality, and where $\mathcal{P}_\delta(x^*) \subset \mathcal{I}_{x^*}$ is the preimage of $B_\delta(x^*) \cap \mathbb{T}_{x^*}\mathcal{I}_{x^*}$ under the projection P restricted to \mathcal{I}_{x^*} .

Now we denote by $x \in \partial\mathcal{I}_{x^*}$ a point in the boundary of \mathcal{I}_{x^*} and, again, $x' = P(x)$. We want to show that the distance $\|a - x\|$ is strictly larger than (13). This would imply that local minimizer for d_a is indeed contained in the interior of $\mathcal{N}_{(x^*, y^*)}$.

We have

$$\begin{aligned}
 \|a - x\| &= \|a - a^* + a^* - x^* + x^* - x' + x' - x\| \\
 &\geq \|a^* - x^* + x^* - x' + x' - x\| - \|a - a^*\|.
 \end{aligned}$$

Note that $x^* = P(a^*)$. Hence we have the orthogonal decomposition

$$a^* - x^* + x^* - x' + x' - x = (\mathbf{1} - P)(a^* - x) + P(a^* - x) = a^* - x.$$

Plugging this into the above, we find

$$\begin{aligned}
 \|a - x\| &\geq \|(\mathbf{1} - P)(a^* - x) + P(a^* - x)\| - \delta = \sqrt{\|(\mathbf{1} - P)(a^* - x)\|^2 + \|P(a^* - x)\|^2} - \delta \\
 &\geq \sqrt{\|(\mathbf{1} - P)(a^* - x)\|^2 + \epsilon^2} - \delta,
 \end{aligned}$$

where $\epsilon = \min_{z \in P(\partial\mathcal{I}_{x^*})} \|x^* - z\| > 0$.

Observe that $a^* - x^*$ is a vector pointing from x^* to a^* and likewise $x' - x$ points from x to x' . Therefore, $\langle a^* - x^*, x' - x \rangle \geq 0$ because both point away from the manifold \mathcal{I}_{x^*} , which lies entirely on the side of x by assumption (ii) above; see also Figure 8. Consequently,

$$\|(\mathbf{1} - P)(a^* - x)\| = \|a^* - x^* + x' - x\| \geq \|a^* - x^*\|.$$

This implies

$$\|a - x\| \geq \sqrt{\|a^* - x^*\|^2 + \epsilon^2} - \delta = \|a^* - x^*\| + \frac{\epsilon^2}{2\|a^* - x^*\|} - \delta + \mathcal{O}(\epsilon^4).$$

Note that h is a continuous function with $\lim_{x \rightarrow x^*} h(x) = 0$. Hence, as $\delta \rightarrow 0$ the maximum height tends to zero as well. Moreover, ϵ and $\|a^* - x^*\|$ are independent

of δ . All this implies that we can choose $\delta > 0$ sufficiently small so that

$$\frac{\epsilon^2}{2\|a^* - x^*\|} - \delta + \mathcal{O}(\epsilon^4) \geq 2\delta + \max_{z \in \mathcal{P}_\delta(x^*)} h(z).$$

It follows that $\|a - x\|$ is lower bounded by (13), so that the minimizer for d_a must be contained in the interior of $\mathcal{N}_{(x^*, y^*)}$.

The foregoing shows that on $B_\delta(a^*) \cap \mathcal{A}_{a^*}$, the map $\Pi_{\mathcal{I}} \circ \Pi_{\mathbb{R}^n}^{-1}$ equals the nonlinear projection $P_{\mathcal{I}_{x^*}}$ onto the manifold \mathcal{I}_{x^*} . Putting everything together, we obtain

$$\rho_{(a^*, x^*, y^*)}(a) = (\Pi_{\mathcal{O}} \circ \Pi_{\mathbb{R}^n}^{-1})(a) = (\pi_{\mathcal{O}} \circ \pi_{\mathcal{I}}^{-1} \circ \Pi_{\mathcal{I}} \circ \Pi_{\mathbb{R}^n}^{-1})(a) = (\pi_{\mathcal{O}} \circ \pi_{\mathcal{I}}^{-1} \circ P_{\mathcal{I}_{x^*}})(a);$$

the second equality following (12). The condition number of this smooth map is given by (2). Comparing with (6) and (9) concludes the proof. \square \square

A.4. Proofs for Section 3.

Proof of Lemma 1. By Corollary 8 the projection $P_{\mathcal{I}} : \mathcal{T} \rightarrow \mathcal{I}$ is a smooth map on \mathcal{T} . Let us denote the graph of this map by $\mathcal{V} := \{(a, P_{\mathcal{I}}(a)) \in \mathcal{T} \times \mathcal{I} \mid a \in \mathcal{T}\}$. It is a smooth embedded submanifold of dimension $\dim \mathcal{T} = \dim \mathcal{N}\mathcal{I} = n$; see, e.g., [25, Proposition 5.4]. Let $x = P_{\mathcal{I}}(a)$, $\eta = a - x$ and $(\dot{a}, \dot{x}) \in T_{(a,x)}\mathcal{V}$ be a nonzero tangent vector. Because of Corollary 8 it satisfies $\dot{x} = (\mathbf{1} - S_\eta)^{-1} P_{T_x \mathcal{I}} \dot{a}$. Hence, $D_{(a,x)} \Pi_{\mathbb{R}^n}(\dot{a}, (\mathbf{1} - S_\eta)^{-1} P_{T_x \mathcal{I}} \dot{a}) = \dot{a} \neq 0$, so that its kernel is trivial. It follows that $\mathcal{V} \subset \mathcal{W}_{\text{CPP}}$. Since their dimensions match by Lemma 2, \mathcal{V} is an open submanifold. As \mathcal{W}_{CPP} is embedded by Lemma 3, \mathcal{V} is embedded as well by [25, Proposition 5.1]. Moreover, by construction, we have

$$\mathcal{W}_{\text{AP}} = (\mathcal{V} \times \mathcal{O}) \cap (\mathbb{R}^n \times \mathcal{W}) \subset \mathbb{R}^n \times \mathcal{I} \times \mathcal{O}.$$

The first part of the proof is concluded by observing that the proof of Lemma 4 applies by replacing \mathcal{W}_{CPP} with \mathcal{V} and $\mathcal{W}_{\text{GCPP}}$ with \mathcal{W}_{AP} .

Finally, we show that \mathcal{W}_{AP} is dense in \mathcal{S}_{AP} . Let $(x + \eta, y) \in \mathcal{S}_{\text{AP}}$ with $x \in \mathcal{I}$ and $\eta \in N_x \mathcal{I}$ be arbitrary. Then $P_{\mathcal{I}}(x + \eta) = x$ and $(x, y) \in \mathcal{S}$. As \mathcal{W} is an open dense submanifold of \mathcal{S} , there exists a sequence $(x_i, y_i) \in \mathcal{W}$ such that $\lim_{i \rightarrow \infty} (x_i, y_i) = (x, y)$. Consider $(x_i + \eta_i, y_i) \in \mathcal{W}_{\text{AP}}$ with $\eta_i \in N_{x_i} \mathcal{I}$ and $\eta_i \rightarrow \eta$ chosen in such a way that the first component lies in the tubular neighborhood; this is possible as \mathcal{T} is an open submanifold of \mathbb{R}^n . Then, the limit of this sequence is $(x + \eta, y)$, concluding the proof. \square \square

Proof of Theorem 1. For $(a, y) \in \mathcal{W}_{\text{AP}}$, let $x = P_{\mathcal{I}}(a)$ and $\eta = a - x$. By [34, Theorem 4.5], $\kappa_{\text{AP}}(a, y) = \|D_a(\pi_{\mathcal{O}} \circ \pi_{\mathcal{I}}^{-1} \circ P_{\mathcal{I}})\|$. Since $(x, y) \in \mathcal{W}$, we know that $D_{(x,y)} \pi_{\mathcal{I}}$ is invertible. Moreover, by Corollary 8 the derivative of the projection $P_{\mathcal{I}} : \mathcal{T} \rightarrow \mathcal{I}$ at a is $D_a P_{\mathcal{I}} = (\mathbf{1} - S_\eta)^{-1} P_{T_x \mathcal{I}}$. Therefore,

$$\kappa_{\text{AP}}(a, y) = \|(D_{(x,y)} \pi_{\mathcal{O}})(D_{(x,y)} \pi_{\mathcal{I}})^{-1} (\mathbf{1} - S_\eta)^{-1}\|.$$

For $(a, y) \in \mathcal{S}_{\text{AP}} \setminus \mathcal{W}_{\text{AP}}$, we have $(x, y) \notin \mathcal{W}$ with $x = P_{\mathcal{I}}(a)$. By definition of \mathcal{W} , this entails that $D_{(x,y)} \pi_{\mathcal{I}}$ is not invertible, concluding the proof. \square \square

REFERENCES

- [1] T. J. Abatzoglou. The minimum norm projection on C^2 manifolds in R^n . *Trans. Amer. Math. Soc.*, 243:115–122, 1978.
- [2] P.-A. Absil, R. Mahony, and R. Sepulchre. *Optimization Algorithms on Matrix Manifolds*. Princeton University Press, 2008.
- [3] P.-A. Absil and J. Malick. Projection-like retractions on matrix manifolds. *SIAM J. Optim.*, 22(1):135–158, 2012.
- [4] L. Ambrosio and C. Mantegazza. Curvature and distance function from a manifold. *J Geom Anal.*, 8, 1998.
- [5] D. Bau and L. N. Trefethen. *Numerical Linear Algebra*. SIAM, 1997.
- [6] L. Blum, F. Cucker, M. Shub, and S. Smale. *Complexity and Real Computation*. Springer-Verlag, New York, 1998.

- [7] P. Breiding and N. Vannieuwenhoven. Convergence analysis of Riemannian Gauss–Newton methods and its connection with the geometric condition number. *Appl. Math. Letters*, 78:42–50, 2018.
- [8] P. Breiding and N. Vannieuwenhoven. A Riemannian trust region method for the canonical tensor rank approximation problem. *SIAM J. Optim.*, 28(3):2435–2465, 2018.
- [9] P. Bürgisser and F. Cucker. *Condition: The Geometry of Numerical Algorithms*. Springer, Heidelberg, 2013.
- [10] N. Chernov and H. Ma. Least squares fitting of quadratic curves and surfaces. In S. Yoshida, editor, *Computer Vision*. Nova Science Publishers, 2011.
- [11] C. Da Silva and F. J. Herrmann. Optimization on the hierarchical Tucker manifold – applications to tensor completion. *Linear Algebra Appl.*, 481:131–173, 2015.
- [12] J. W. Demmel. The geometry of ill-conditioning. *J. Complexity*, 3(2):201–229, 1987.
- [13] J. W. Demmel. On condition numbers and the distance to the nearest ill-posed problem. *Numer. Math.*, 51(3):251–289, 1987.
- [14] M. do Carmo. *Riemannian Geometry*. Birkhäuser, 1993.
- [15] J. Draisma, E. Horobet, G. Ottaviani, B. Sturmfels, and R. Thomas. The euclidean distance degree of an algebraic variety. *Foundations of Computational Mathematics*, 16(1):99–149, 2016.
- [16] E. Dudek and K. Holly. Nonlinear orthogonal projection. *Ann. Pol. Math.*, 59:1–31, 1994.
- [17] O. Faugeras and Q. Luong. *The Geometry of Multiple Images*. MIT Press, Cambridge, MA, 2001. The laws that govern the formation of multiple images of a scene and some of their applications, With contributions from Théo Papadopoulos.
- [18] R. Hartley and A. Zisserman. *Multiple View Geometry in Computer Vision*. Cambridge University Press, Cambridge, second edition, 2003. With a foreword by Olivier Faugeras.
- [19] A. Heyden and K. Åström. Algebraic properties of multilinear constraints. *Math. Meth. Appl. Sci.*, 20:1135–1162, 1997.
- [20] N. Higham. *Accuracy and Stability of Numerical Algorithms*. SIAM, Philadelphia, PA, 1996.
- [21] M. W. Hirsch. *Differential Topology*. Number 33 in Graduate Text in Mathematics. Springer-Verlag, 1976.
- [22] D. Kressner, M. Steinlechner, and B. Vandereycken. Low-rank tensor completion by Riemannian optimization. *BIT Numer. Math.*, 54(2):447–468, 2014.
- [23] Z. Kúkelová. *Algebraic Methods in Computer Vision*. PhD thesis, Czech Technical University in Prague, 2013.
- [24] J. M. Lee. *Riemannian Manifolds: Introduction to Curvature*. Springer Verlag, 1997.
- [25] J. M. Lee. *Introduction to Smooth Manifolds*. Springer, New York, USA, 2 edition, 2013.
- [26] G. Leobacher and A. Steinicke. Existence, uniqueness and regularity of the projection onto differentiable manifolds. *arXiv:1811.10578v3*, 2019.
- [27] Y. Liu and W. Wang. A revisit to least squares orthogonal distance fitting of parametric curves and surfaces. In F. Chen and B. Juttler, editors, *Advances in Geometric Modeling and Processing*. Lecture Notes in Computer Science, 2008.
- [28] MATLAB. R2017b. Natick, Massachusetts, 2017.
- [29] S. Maybank. *Theory of Reconstruction from Image Motion*, volume 28 of *Springer Series in Information Sciences*. Springer-Verlag, Berlin, 1993.
- [30] B. O’Neill. *Semi-Riemannian Geometry*. Academic Press, 1983.
- [31] B. O’Neill. *Elementary Differential Geometry*. Elsevier, revised second edition edition, 2001.
- [32] P. Petersen. *Riemannian Geometry*, volume 171 of *Graduate Texts in Mathematics*. Springer, New York, second edition, 2006.
- [33] I. R. Porteous. The normal singularities of a submanifold. *J. Differential Geometry*, 5, 1971.
- [34] J. R. Rice. A theory of condition. *SIAM J. Numer. Anal.*, 3(2):287–310, 1966.
- [35] M. Shub and S. Smale. Complexity of Bézout’s theorem. I. Geometric aspects. *J. Amer. Math. Soc.*, 6(2):459–501, 1993.
- [36] M. Shub and S. Smale. Complexity of Bezout’s theorem. II. Volumes and probabilities. In *Computational algebraic geometry (Nice, 1992)*, volume 109 of *Progr. Math.*, pages 267–285. Birkhäuser Boston, Boston, MA, 1993.
- [37] M. Shub and S. Smale. Complexity of Bezout’s theorem. III. Condition number and packing. *J. Complexity*, 9(1):4–14, 1993.
- [38] M. Shub and S. Smale. Complexity of Bezout’s theorem. V. Polynomial time. *Theoret. Comput. Sci.*, 133(1):141–164, 1994.
- [39] M. Shub and S. Smale. Complexity of Bezout’s theorem. IV. Probability of success; extensions. *SIAM J. Numer. Anal.*, 33(1):128–148, 1996.
- [40] M. Spivak. *A Comprehensive Introduction to Differential Geometry*, volume 2. Publish or Perish, Inc., 1999.
- [41] M. Steinlechner. Riemannian optimization for high-dimensional tensor completion. *SIAM J. Sci. Comput.*, 38:S461–S484, 2016.

- [42] A. Sung-Joon. Geometric fitting of parametric curves and surfaces. *J. Information Processing Systems*, 4(4):153–158, 2008.
- [43] R. Thom. Sur la theorie des enveloppes. *J. Math. Pures Appl.*, 41:177–192, 1962.
- [44] B. Vandereycken. Low-rank matrix completion by Riemannian optimization. *SIAM J. Optim.*, 23(2):1214–1236, 2013.
- [45] Visual Geometry Group, University of Oxford. Model house data set, Last accessed 19 september 2019. Access online at <https://www.robots.ox.ac.uk/~vgg/data/data-mview.html>.
- [46] H. Weyl. On the volume of tubes. *Amer. J. Math.*, 2:461–472, 1939.
- [47] J. H. Wilkinson. *Rounding Errors in Algebraic Processes*. Prentice-Hall, Englewood Cliffs, New Jersey, 1963.
- [48] H. Woźniakowski. Numerical stability for solving nonlinear equations. *Numer. Math.*, 27(4):373–390, 1976/77.